



# Soil chemistry, temperature and bacterial community composition drive brGDGT distributions along a subarctic elevation gradient

Robin Halfman<sup>a</sup>, Jonas Lembrechts<sup>a</sup>, Dajana Radujković<sup>a</sup>, Johan De Gruyter<sup>a</sup>, Ivan Nijs<sup>a</sup>,  
Cindy De Jonge<sup>a,b,\*</sup>

<sup>a</sup> University of Antwerp, Dept. of Biology, Universiteitsplein 1, 2610 Wilrijk, Belgium

<sup>b</sup> ETH Zürich, Geological Institute, Sonneggstrasse 5, 8092 Zürich, Switzerland

## ARTICLE INFO

Associate Editor—Johan Weijers

### Keywords:

brGDGT  
Biomarker proxy  
Bacterial community  
Soil biomarkers

## ABSTRACT

Branched glycerol dialkyl glycerol tetraethers (brGDGTs) are bacterial membrane lipids which can be used to reconstruct past terrestrial mean annual air temperature (MAAT) and soil pH values. To reconstruct these environmental conditions in geological archives, we make use of the brGDGT ratios MBT<sub>5ME</sub>, CBT<sup>+</sup> and IR, which summarize the structural variation in brGDGT lipids. However, the most recent calibrations between the brGDGT-based temperature proxy MBT<sub>5ME</sub> and temperature on a global scale are characterized by a residual error between 3.8 °C and 6.0 °C. This lack of accuracy of the MBT<sub>5ME</sub>-MAAT calibration is often attributed to the difference between soil and atmospheric temperatures. Also, previous studies suggested that the variation of the MBT<sub>5ME</sub> along chemistry and temperature gradients reflects a possible influence of bacterial community changes. Here, we analyzed the effect environmental variables have on brGDGT signatures collected along five elevation gradients in the north of Sweden and Norway, where MAAT changed between -4.7 °C and 2.7 °C and soil pH varies between 3.3 and 5.7. Specifically, we determined the impact of air and soil temperature, the bacterial community composition and soil chemical characteristics. The range of MBT<sub>5ME</sub> values encountered (0.30–0.70) results in a wide range of reconstructed temperatures (1–13 °C). The use of in situ soil temperature data spanning one year did not improve the correlation with brGDGT MBT<sub>5ME</sub> values, compared to using a long-term MAAT dataset. Although a temperature gradient was present, soil chemistry apparently determined brGDGTs concentration and distribution on this local scale. Specifically, soils with high cation exchange capacity (CEC) showed an increased concentration of brGDGT Ia, resulting in increased Community Index (CI) and MBT<sub>5ME</sub> values, both brGDGT ratios that reflect the degree of methylation. Soils with increased pH (pH range 5–6) had a distinct brGDGT fingerprint with generally decreased MBT<sub>5ME</sub> values, which resulted in the correlation between MBT<sub>5ME</sub> and soil pH ( $r = -0.60$ ,  $p < 0.01$ ). Contrary to expectations, pH was a better predictor of MBT<sub>5ME</sub> values than temperature ( $r = 0.47$ ,  $r = 0.44$ ,  $p < 0.01$ , with MAAT and mean summer soil temperature (MSST), respectively). Soil pH also shaped the bacterial community composition, and a bio-indicator approach was used to narrow down the proposed bacterial producer of brGDGT lipids in high CI (Acidobacteria subgroups 1 and 3) and high pH soils (Acidobacteria subgroups 6 and 7). Building upon previous research, this confirms that brGDGTs respond to similar changes in bacterial community composition across sites. Because of the interplay between temperature and soil chemistry, the relationship between the MBT<sub>5ME</sub> and soil temperature is clearly complex at the local scale. Further disentangling these environmental drivers is still essential in the development of the MBT<sub>5ME</sub> proxy as paleothermometer.

## 1. Introduction

Quantitative paleoclimate reconstructions can significantly improve models that constrain climate sensitivity (Tierney et al., 2020). BrGDGTs (branched glycerol dialkyl glycerol tetraethers) show great potential as

quantitative paleoclimate indicators in paleosoils, lake and near-shore marine sediments (Schouten et al., 2013), where they are stable over long geological timescales (up to 200 Ma; O'Brien et al., 2017). Produced by bacteria as membrane-spanning lipids, 15 different structures are used in paleoclimate proxies. The core consists of two straight alkyl

\* Corresponding author at: Sonneggstrasse 5 – NO G 57, 8092 Zurich, Switzerland.

E-mail address: [cindy.dejonge@erdw.ethz.ch](mailto:cindy.dejonge@erdw.ethz.ch) (C. De Jonge).

<https://doi.org/10.1016/j.orggeochem.2021.104346>

Received 25 August 2021; Received in revised form 22 October 2021; Accepted 21 November 2021

Available online 27 November 2021

0146-6380/© 2021 The Author(s).

Published by Elsevier Ltd.

This is an open access article under the CC BY-NC-ND license

(<http://creativecommons.org/licenses/by-nc-nd/4.0/>).

chains, each comprising two to three methyl groups (Supplementary Fig. S1). Following internal cyclization, a cyclopentane moiety can be present on each alkyl chain (Schouten et al., 2000; Sinninghe Damsté et al., 2000; Weijers et al., 2006). The outer branch can be located on the  $\alpha$  and/or  $\omega$ -5 or  $\omega$ -6 position (so-called 5-methyl and 6-methyl brGDGTs; De Jonge et al., 2013). On a global scale, the distribution of brGDGT lipid in soils changes with mean annual air temperature (MAAT) and soil pH (Weijers et al., 2007; De Jonge et al., 2014a, Naafs et al., 2017a, 2017b, Dearing Crampton-Flood et al., 2020). Specifically, the degree of methylation of 5-methyl brGDGTs (summarized as the  $MBT'_{5ME}$  ratio (De Jonge et al., 2014a)) has been shown to vary with air temperature. The relative amount of cyclized and 6-methyl brGDGTs (summarized as the CBT' ratio; De Jonge et al., 2014a) varies according to pH values. Similar ratios, such as the isomer ratio (IR; De Jonge et al., 2014b; Yang et al., 2015) and degree of cyclizations (DC'; modified after Sinninghe Damsté et al., 2009) have been developed to trace changes in pH.

Recently, the biochemical response mechanism of the environmental sensitivity of the brGDGT ratios has been revisited. Weijers et al. (2007) initially hypothesized that an unchanged community of bacterial producers changed the composition of their cell membrane to counteract the impact of temperature and soil pH on membrane fluidity and functioning. This is supported by membrane lipid simulations that show that increasing the degree of methylation render the membrane less rigid and more fluid (Naafs et al., 2021). However, the strong pH dependency of 6-methyl brGDGTs (De Jonge et al., 2014a), could not be easily explained by a change in membrane permeability for  $H^+$  ions. The impact of the incorporation of 6-methyl brGDGTs on a membrane structure has not been tested, but is expected to be minor, as they are structurally very similar to their 5-methyl counterparts.

Sinninghe Damsté et al. (2011, 2014, 2018) reported that the presence of different proposed brGDGT precursor compounds in Acidobacterial cultures, so-called *iso*-diabiotic acid (IDA), 6-methyl IDA and mono-glycerol-ether (MGE-IDA), reflect the phylogenetic position of these cultures. This indicates that the potential to produce brGDGT lipids is pre-determined for different Acidobacterial subgroups. Initial environmental studies, where the composition of brGDGTs and bacterial communities along environmental gradients are compared, support this hypothesis. Along geothermally heated soils, drastic bacterial community composition changes have been shown to co-occur with a stepwise change in the  $MBT'_{5ME}$  ratio (De Jonge et al., 2019). The lipid distribution that reflects this change in bacterial community, the so-called Community Index (CI), allows one to extrapolate this effect on a global scale, dividing soils between a "Cluster Warm" and "Cluster Cold" based on their lipid distribution. These authors postulated that the globally observed temperature dependency of the  $MBT'_{5ME}$  ratio, is caused at least in part by a change in the composition of the bacterial producers. However, on a global scale there is no clear temperature threshold between the "Cluster Warm" and "Cluster Cold" soils, indicating the temperature is not the only factor determining the presence of either community. Another environmental study used grassland and agricultural sites where natural pH changes were present or where pH gradients were artificially established (De Jonge et al., 2021). The presence of alkalinity-promoted compounds (i.e. brGDGTs Ib, Ic, Iib, Iic, IIb, IIc, IIIa, IIIb, IIIc) was coeval with a change in the composition of soil bacteria (De Jonge et al., 2021).

Both temperature and pH-driven changes in the bacterial community composition are thus proposed to impact the  $MBT'_{5ME}$  values. While this previous research outlines the initial evidence that bacterial community changes drive the concentration and distribution of brGDGTs as well as their climate proxy ratios, the extent of this effect along elevation gradients that represent natural changes in temperature and soil chemistry, remains to be confirmed. Here, we discuss the distribution of brGDGT lipids along elevation gradients (13.8–1186 m asl) in northern Sweden and Norway and determine the effect of naturally occurring changes in air and soil temperature and soil chemistry on brGDGTs and their potential bacterial producers. With in situ measured soil temperature data

along such a clear environmental gradient (noteworthy different from coarse-grained air temperatures and more relevant for belowground processes (Lembrechts et al., 2016, 2020)), we expected to find strong correlations between temperature and brGDGTs, coinciding with changes in bacterial communities. However, the range in  $MBT'_{5ME}$  values was much larger than expected, showing only a weak correlation with temperature parameters. This was explained by the strong impact of soil chemistry (pH, CEC, exchangeable Ca) on brGDGT concentrations and fractional abundances. We confirm that bacterial community changes occur both in soils with increased CI and  $MBT'_{5ME}$  values, decreased brGDGT Ia and  $MBT'_{5ME}$  values, and in soils with increased amounts of brGDGT IIIa and 6-methyl brGDGTs. These changes explain the large variation in  $MBT'_{5ME}$  values and the poor correlation with temperature at this site.

## 2. Material and methods

### 2.1. Soil sampling

The sampling locations (Fig. 1) were situated in the Scandinavian Mountains in the north of Sweden and Norway, 160 km north of the Arctic Circle, between N 67°46'23.5"/E 16°30'52.6" (southwest) and N 68°40'33.6"/E 18°58'40.4" (northeast). The sampling sites were located in natural vegetation along two mountain trails and three mountain roads, with altitudes ranging from near sea level (13.6 m asl) to almost 1200 m asl (Fig. 1). Table 1 lists the coordinates and altitude of the sampling sites, that are part of a framework of long-term vegetation survey plots (Lembrechts et al., 2019) of the Mountain Invasion Research Network (MIREN; Haider et al., 2021). The sites were located 50 m from the roadside or 10 m from the trailside, beyond the disturbance effect (Lembrechts et al., 2016) and each soil sample collected was located next to a soil temperature sensor (distance = 5–100 cm, depending on the availability of soil). Surface soil samples (n = 37) were taken between 16th and 30th of July 2018. Each sample consisted of a composite of four soil cores ( $\phi$  2 cm), taken within a 1 m radius, collecting the top 5 cm of the soil. Samples were stored in aluminum foil and stored frozen until analysis.

### 2.2. Temperature data and chemical analysis of soils

Soil temperature data were collected using iButtons, (DS1922L, Maxim Integrated, www.maximintegrated.com, San José, CA, USA) that were covered in Parafilm to protect against moisture and buried at approximately 2 cm depth. The collected soil temperature spans the period from 16/07/2017 to 15/07/2018, with a measurement interval of 60 min (Fig. 1). Based on the soil measurements taken, the following temperature parameters have been calculated: (i) mean annual soil temperature (MAST): the average soil temperature ( $^{\circ}C$ ) at the sampling site measured over the whole period, (ii) mean summer soil temperature (MSST): the average soil temperature ( $^{\circ}C$ ) at the sampling site measured during the warmest quartile (July to September) and (iii) growing degree days (GDD): an ecologically relevant measure of heat accumulation, calculated as the sum of all degrees ( $^{\circ}C$ ) on days that the daily average temperature was above  $0^{\circ}C$  during the whole measurement period (Table 1) (Lembrechts et al., 2016). In addition, mean annual air temperatures (MAAT) were extracted from the CHELSA climate database (Karger et al., 2017), that has a resolution of 30 arc sec ( $\sim 1$  km), which covers the period from 1979 to 2013 (Table 1).

Soil pH was measured in the lab using a calibrated pH meter (Hanna instruments; HI 99121) in demineralized water to soil ratio of 1:2.5 (v/v) (Table 1 and Supplementary Table S1). Exchangeable cation concentrations ( $meq.100\ g^{-1}$ ) were analyzed using a protocol modified from van Reeuwijk (2002). The total levels of different ions in the soils (Supplementary Table S1,  $mg.kg^{-1}$ ) were determined after acid digestion using sulfuric acid ( $H_2SO_4$ ), salicylic acid ( $C_7H_6O_3$ ), hydrogen peroxide ( $H_2O_2$ ) and selenium following a protocol from Novozamsky

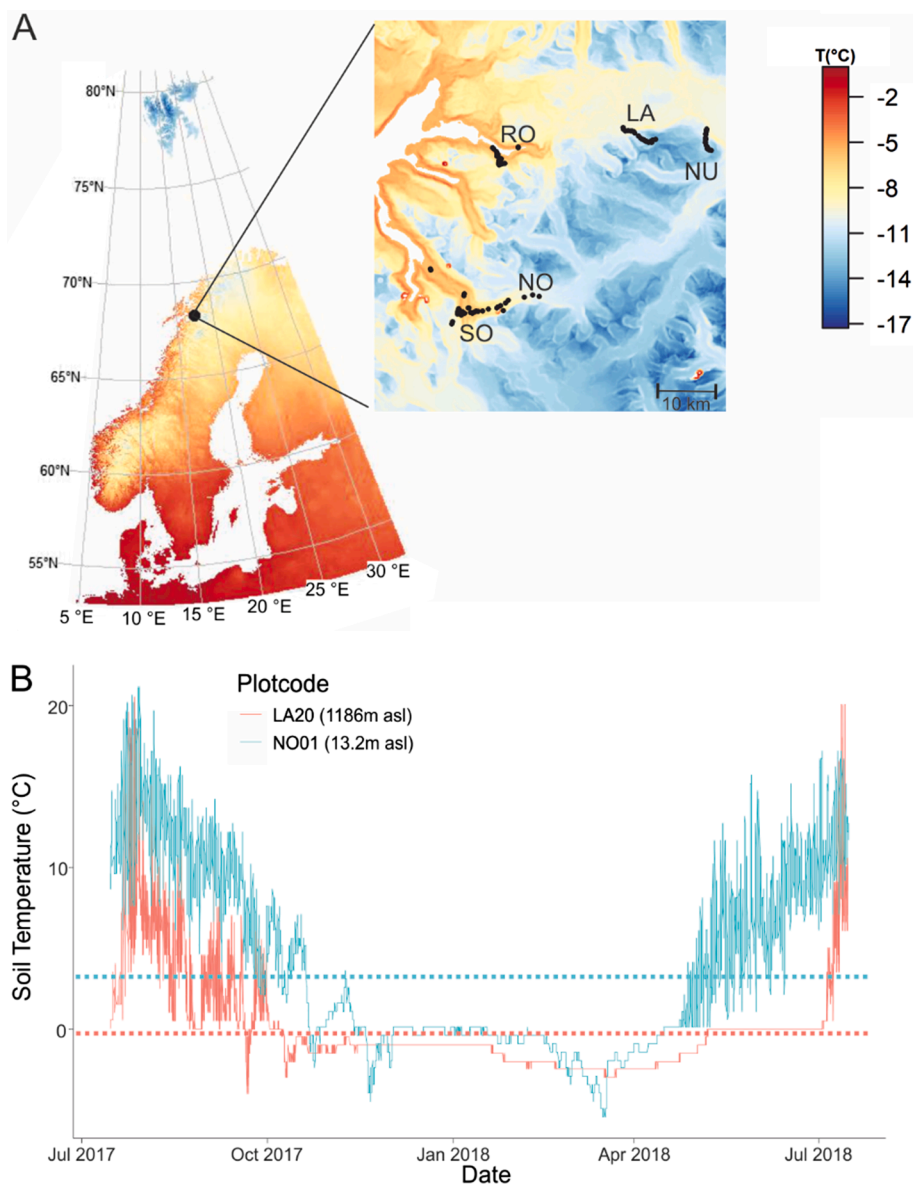


Fig. 1. (A) Study site and transect location (insert, soil sites indicated with black points) in Northern Europe. Background colors indicate mean annual air temperatures. (B) Yearly evolution of soil temperature values at 2 sites (NO01 and LA20) is plotted, with the mean annual soil temperature indicated with a dotted line.

et al. (1983), modified by Walinga et al. (1995). Exchangeable ( $\text{Ca}^{2+}$ ,  $\text{K}^+$ ,  $\text{Mg}^{2+}$ ,  $\text{Mn}^{2+}$ ,  $\text{Fe}^{2+}$ ,  $\text{Na}^+$ ,  $\text{Al}^{3+}$ ) and total cations (P, N,  $\text{Ca}^{2+}$ ,  $\text{K}^+$ ,  $\text{Mg}^{2+}$ ,  $\text{Na}^+$ ) were analyzed using IPC-OES (Inductive Coupled Plasma - Optical Emission Spectrometry) and reported in Supplementary Table S1. Free acidity was analyzed using a method based on Brown (1943). From the concentration of the free ions we calculated the cation exchange capacity ( $\text{CEC} = \text{Exch.} (\text{Na} + \text{K} + \text{Ca} + \text{Mg} + \text{acidity})$ ) and the percentage of available cations consisting out of bases, (base saturation (%)) =  $(\text{Exch.} (\text{Ca} + \text{Mg} + \text{K} + \text{Na}) / \text{CEC}) \times 100$ .

### 2.3. Lipid analysis and calculation of lipid proxies

Lipids were extracted from 2.4 to 5 g of freeze-dried soil sample using a modified Bligh and Dyer method as described by Pitcher et al. (2009). The samples were submerged in a mixture of MeOH/dichloromethane (DCM)/phosphate buffer (2:1:0.8, v/v/v) and ultrasonically extracted ( $3 \times$ ) for 10 min. The total lipid extract was separated into an apolar lipid fraction, a keto fraction and a polar lipid fraction over a small aluminum oxide column, using *n*-hexane/DCM (9:1, v/v), *n*-hexane/DCM (1:1, v/v) and DCM/methanol (1:1, v/v), respectively. The polar fraction,

containing core lipid brGDGTs, was filtered using a 0.45  $\mu\text{m}$  PTFE filter prior to analysis using high-performance liquid chromatography-atmospheric pressure chemical ionization-mass spectrometry (HPLC-APCI-MS), as described by Hopmans et al. (2016). Detection was achieved in selected ion monitoring mode (SIM; Schouten et al., 2007a) using  $m/z$  744 for the internal standard,  $m/z$  1292 for crenarchaeol and  $m/z$  1050, 1048, 1046, 1036, 1034, 1032, 1022, 1020 and 1018 for branched GDGTs. Agilent Chemstation software was used to integrate peak areas in the mass chromatograms of the protonated molecule ( $(\text{M} + \text{H})^+$ ). Filtration, detection and integration of the peak areas was done at Utrecht University (NL). Where a brGDGT compound was encountered below the detection limit, its concentration is reported as “not available”, and the fractional abundance is reported as 0. Table 2 reports the fractional abundances of the 15 brGDGT compounds that are used to calculate brGDGT ratios MBT<sub>5ME</sub>, CBT' (De Jonge et al., 2014a), IR (De Jonge et al., 2014b) and DC' (Sinninghe Damsté et al., 2009) (Eqs. (1)–(4)), as well as a reconstructed MAAT and pH based on global scale relationships (Eqs. (5) and (6)) (De Jonge et al., 2014a). These ratios were calculated using the brGDGTs measured along the altitudinal transects. To situate the variability in the encountered ratio values, we

**Table 1**

Site names, coordinates and altitude above sea level (asl), temperature parameters (mean annual air temperature (MAAT), mean annual soil temperature (MAST), mean summer soil temperature (MSST) and growing degree days (GDD)), and soil pH).

Site	Latitude (°N)	Longitude (°E)	Elevation (masl)	MAAT (°C)	MAST (°C)	MSST (°C)	GDD (°C)	pH
NO01	68.238157	17.427843	13.2	2.7	3.2	10.4	1254	4.5
NO07	68.160694	17.589851	225.9	-0.6	3.2	11.0	1428	4.4
NO10	68.160143	17.622582	332.4	-1.4	2.5	9.9	1194	4.5
NO14	68.165738	17.699969	466.5	-1.0	3.0	9.2	1018	4.3
NO16	68.169281	17.721910	534.7	-2.6	1.6	8.4	921	3.8
NO19	68.175356	17.842269	642	-1.6	1.9	10.6	1311	4.4
RO02	68.420113	17.759362	43.2	2.3	1.3	9.1	875	5.0
RO04	68.416771	17.766323	103.3	1.4	2.9	11.3	1391	4.4
RO06	68.412627	17.773819	166.4	1.9	3.3	9.1	1140	4.8
RO09	68.407690	17.775843	256.1	0.9	3.1	9.7	1184	4.8
RO10	68.407942	17.770727	292.2	0.5	3.1	10.0	1109	4.9
RO12	68.401289	17.778477	352.9	-0.2	2.8	10.2	1182	5.4
RO19	68.394523	17.789341	565	-2.0	1.2	10.2	1065	5.0
SO03	68.168447	17.563202	80.9	2.1	4.3	11.3	1482	4.5
SO05	68.161449	17.538411	152.7	1.7	3.2	10.3	1246	5.2
SO09	68.158860	17.532130	275.4	0.9	2.7	12.3	1602	4.2
SO13	68.164552	17.526290	399.3	0.9	2.5	12.6	1678	4.8
SO17	68.163864	17.518161	527.5	0.0	2.9	9.8	1135	4.9
SO20	68.146025	17.484477	634.7	-0.6	1.1	6.0	533	5.2
LA02	68.422550	18.325376	579	-1.1	1.7	8.0	741	3.3
LA05	68.418290	18.353724	620	-3.2	1.1	5.3	339	5.1
LA08	68.414331	18.369071	738	-2.6	1.3	7.1	536	5.5
LA10	68.403966	18.392049	812	-3.0	0.4	6.8	609	4.6
LA12	68.400909	18.403174	890	-3.8	1.0	6.7	617	5.6
LA15	68.397081	18.416653	965	-3.7	-1.2	6.8	612	5.2
LA16	68.395698	18.423913	997	-4.0	-2.5	5.5	510	4.8
LA18	68.397706	18.437351	1089	-4.2	0.9	6.7	570	5.0
LA20	68.398335	18.454618	1186	-4.7	-0.2	4.0	279	4.8
NU01	68.402892	18.677607	428	-1.1	2.8	8.9	974	5.7
NU03	68.400658	18.674642	469	-1.1	2.2	8.9	894	5.4
NU08	68.387715	18.667869	646	-2.0	-0.1	6.8	711	4.5
NU10	68.385023	18.665959	716	-2.5	0.1	7.7	759	5.2
NU11	68.381623	18.662820	749	-2.4	2.1	8.2	875	4.5
NU13	68.372865	18.668659	824	-3.0	-2.2	7.1	761	4.5
NU15	68.370771	18.668143	887	-3.0	0.7	7.3	696	5.7
NU17	68.369219	18.673102	956	-4.2	0.0	6.2	605	5.4
NU18	68.368662	18.675416	998	-4.2	-2.2	6.3	616	5.2

compared them with an extended global soil dataset. This dataset is a compilation of brGDGT distributions previously reported in De Jonge et al. (2014a), Ding et al. (2015), Xiao et al. (2015), Yang et al. (2015), Lei et al. (2016), and Naafs et al. (2017a,b). The roman numerals below refer to the brGDGT structures as shown in Supplementary Fig. S1. To differentiate between 5- and 6-methyl brGDGTs, the latter are indicated by a prime symbol.

$$MBT_{SME}^* = (Ia + Ib + Ic) / (Ia + Ib + Ic + IIa + IIb + IIc + IIIa) \quad (1)$$

$$CBT^* = \log_{10}((Ic + IIa' + IIb' + IIc' + IIIa' + IIIb' + IIIc') / (Ia + IIa + IIIa)) \quad (2)$$

$$IR = (IIa' + IIIa') / (IIa + IIIa + IIa' + IIIa') \quad (3)$$

$$DC^* = (Ib + IIb + IIb') / (Ia + IIa + IIa' + Ib + IIb + IIb') \quad (4)$$

$$MAT = -8.57 + 31.45 \times MBT_{SME}^* \quad (5)$$

$$pH = 7.15 + 1.59 \times CBT^* \quad (6)$$

Following the development of brGDGT ratios that allow empirical relationships with temperature and pH on a global scale, a ratio has recently been proposed to reflect bacterial community changes along a geothermal gradient. The community index (CI; De Jonge et al., 2019) was developed to distinguish between “Cluster Cold” and “Cluster Warm” lipid distributions, supposedly produced by different brGDGT-producing soil communities.

$$CI = Ia / (Ia + IIa + IIIa) \quad (7)$$

#### 2.4. DNA extraction and analysis

DNA was isolated from 0.25 to 0.35 g of soil according to the manufacturer's protocol of the DNeasy PowerSoil kit (Qiagen, the Netherlands). Prior to DNA amplification, the extracts were purified from inhibitors using the Zymo inhibitor removal kit (Zymo Research corp., USA; Stevenson, 1982). The V4 region of 16 s rRNA gene was amplified using 515F and 806r primers (Caporaso et al., 2011), amended with Illumina Nextera labels (Illumina Inc; San Diego, CA, USA) during the first PCR. Each 25 µl reaction mixture contained 1 µl of the sample, 0.5 µM of each forward and reverse primer, 1 × PCR buffer, 200 µM dNTPs and 1 U Phusion High-Fidelity DNA polymerase (New England Biolabs, Ipswich, MA, USA). PCR conditions were as follows: initial denaturation at 98 °C for 60 s, followed by 25 cycles of: denaturation at 98 °C for 30 s, annealing at 55 °C for 30 s, extension at 72 °C for 30 s; and an additional extension of 72 °C for 10 min. A second PCR was performed, adding index adapters to each extremity of the PCR products. For this, we used dual barcoded primers with Illumina adapters (2.5 µl of 50 × diluted PCR products template and 0.1 µM of each primer). The conditions for the second PCR were: 98 °C for 60 s, 12 cycles: at 98 °C for 10 s, 63 °C for 30 s, 72 °C for 30 s; and a final step at 72 °C for 5 min. PCR products were run on an agarose gel to confirm successful PCR amplification and successful amplicons were normalized and purified from primers and primer-dimers using the SequalPrep Normalization Plate Kit (ThermoFisher Scientific).

Samples that failed to produce PCR product were subject to repeated soil extraction and PCR. However, for 11 samples, DNA extraction and amplification was not successful, four samples from section LA (LA8,

**Table 2**  
 Fractional abundance (%) of 13 brGDGTs is reported, as well as summed concentration (ng·g<sup>-1</sup> soil). BrGDGT-based climate ratios (MBT<sub>5ME</sub>, CBT', IR, DC') as well as reconstructed MAAT (based on MBT<sub>5ME</sub>) and pH (based on CBT' and proposed brGDGT-based community index CI).

Site	BrGDGT fractional abundance (%)													brGDGT ng·g <sup>-1</sup> soil	MBT <sub>5ME</sub>	CBT'	DC'	IR	CI	MAT <sub>rec</sub> (°C)	pH <sub>rec</sub>
	Ia	Ib	Ic	IIa	IIb	IIc	IIIa	IIIb	IIIc	IIa'	IIb'	IIIa'	IIIb'								
NO01	59.7	0.9	0.3	32.8	0.6	0.5	4.6	0.04	0.04	0.5	0.02	0.2	b.d.l.	271	0.61	-2.03	0.02	0.02	0.61	10.7	3.9
NO07	51.5	1.3	0.5	35.8	0.9	0.7	5.5	b.d.l.	b.d.l.	3.0	0.3	0.6	b.d.l.	769	0.55	-1.33	0.03	0.08	0.56	8.9	5.0
NO10	47.3	0.9	0.2	43.0	0.5	0.4	7.1	0.02	0.02	0.4	0.1	b.d.l.	b.d.l.	1021	0.49	-2.11	0.02	0.01	0.49	6.7	3.8
NO14	46.4	1.4	0.4	41.8	0.8	0.6	8.3	0.04	0.05	b.d.l.	b.d.l.	0.3	0.02	1784	0.48	-2.13	0.02	0.01	0.48	6.6	3.8
NO16	68.2	0.9	0.2	27.6	0.4	0.3	2.1	0.02	0.01	b.d.l.	b.d.l.	0.1	0.01	5395	0.69	-2.43	0.01	0.00	0.70	13.3	3.3
NO19	53.1	0.6	0.2	38.9	0.4	0.4	5.3	0.03	0.02	0.9	b.d.l.	0.2	b.d.l.	2628	0.54	-1.9	0.01	0.02	0.55	8.5	4.1
RO02	59.4	0.7	0.3	34.2	0.5	0.6	3.9	b.d.l.	b.d.l.	0.4	b.d.l.	0.1	b.d.l.	111	0.61	-2.09	0.01	0.01	0.61	10.5	3.8
RO04	50.1	1.0	0.3	39.7	0.7	0.6	5.9	0.06	0.04	1.3	b.d.l.	0.3	b.d.l.	517	0.52	-1.69	0.02	0.03	0.52	7.9	4.5
RO06	55.2	1.2	0.3	36.5	0.5	0.5	5.5	0.03	0.03	b.d.l.	b.d.l.	0.2	0.02	1672	0.57	-2.27	0.02	0.00	0.57	9.3	3.5
RO09	47.2	1.4	0.4	39.6	0.9	0.7	7.3	0.05	0.04	2.0	0.02	0.4	0.02	1451	0.5	-1.51	0.03	0.05	0.50	7.2	4.7
RO10	54.0	2.5	0.4	34.2	0.6	0.3	5.2	0.04	b.d.l.	2.3	b.d.l.	0.3	0.01	688	0.59	-1.5	0.03	0.06	0.58	9.8	4.8
RO12	31.7	1.0	0.2	40.0	0.6	0.3	23.7	0.1	0.08	1.8	0.05	0.5	0.08	1414	0.34	-1.57	0.02	0.03	0.33	2.0	4.7
RO19	33.1	0.7	0.2	37.6	0.3	0.2	23.2	0.04	b.d.l.	3.4	0.2	0.9	0.3	205	0.36	-1.29	0.02	0.06	0.35	2.7	5.1
SO03	40.8	1.4	0.2	41.5	0.8	0.3	12.9	0.07	0.02	1.5	0.03	0.4	0.03	1248	0.43	-1.65	0.03	0.03	0.43	5.0	4.5
SO05	35.2	1.3	0.2	37.6	0.7	0.2	19.3	0.06	0.02	4.4	0.08	0.9	0.04	914	0.39	-1.21	0.03	0.09	0.38	3.6	5.2
SO09	64.3	3.9	0.6	26.3	0.6	0.4	3.0	b.d.l.	b.d.l.	0.9	0.03	0.1	b.d.l.	6761	0.69	-1.77	0.05	0.03	0.69	13.3	4.3
SO13	48.5	1.3	1.3	40.4	b.d.l.	b.d.l.	8.5	b.d.l.	b.d.l.	b.d.l.	b.d.l.	b.d.l.	b.d.l.	260	0.51	-1.87	0.01	0.00	0.50	7.5	4.2
SO17	46.1	1.1	0.2	37.2	0.5	0.3	10.1	0.05	0.05	3.9	0.1	0.5	0.09	372	0.5	-1.3	0.02	0.08	0.49	7.0	5.1
SO20	32.6	0.8	0.2	35.4	0.3	0.1	22.7	0.1	0.04	5.7	0.2	1.7	0.2	126	0.36	-1.06	0.02	0.11	0.36	2.9	5.5
LA02	50.5	1.2	0.2	37.1	0.6	0.4	7.2	0.04	0.02	2.4	0.1	0.2	b.d.l.	921	0.53	-1.5	0.02	0.06	0.53	8.2	4.8
LA05	45.5	3.5	0.4	34.8	0.9	0.4	12.5	0.04	0.03	1.7	0.02	0.2	0.03	685	0.5	-1.59	0.05	0.04	0.49	7.3	4.6
LA08	38.1	1.2	0.2	40.5	0.5	0.3	17.8	0.03	b.d.l.	0.5	0.07	0.6	0.05	741	0.4	-1.82	0.02	0.02	0.40	4.0	4.3
LA10	48.5	0.4	0.2	39.5	0.4	0.3	10.7	0.06	b.d.l.	b.d.l.	b.d.l.	b.d.l.	b.d.l.	574	0.49	-2.81	0.01	0.00	0.49	6.9	2.7
LA12	30.9	3.4	0.5	39.1	0.1	0.7	17.1	0.1	0.05	6.5	0.01	1.5	0.08	2161	0.38	-1.01	0.04	0.12	0.35	3.3	5.6
LA15	43.7	1.2	0.2	40.3	0.4	0.3	11.9	0.05	0.06	1.6	b.d.l.	0.3	0.03	264	0.46	-1.65	0.02	0.04	0.46	5.9	4.5
LA16	34.5	0.2	0.1	46.9	0.2	0.1	17.2	0.04	b.d.l.	0.5	b.d.l.	0.3	b.d.l.	436	0.35	-2.09	0	0.01	0.35	2.4	3.8
LA18	33.2	0.5	0.1	35.6	0.5	0.2	22.8	0.08	0.1	5.3	0.08	1.5	0.1	255	0.36	-1.11	0.01	0.10	0.36	2.9	5.4
LA20	35.9	0.5	0.1	44.2	0.2	0.2	18.2	0.03	0.02	0.5	b.d.l.	0.2	b.d.l.	1125	0.37	-2.09	0.01	0.01	0.36	3.0	3.8
NU01	27.8	1.1	0.4	38.6	0.9	0.3	26.7	0.08	0.05	2.8	0.2	1.1	0.06	2013	0.31	-1.32	0.03	0.06	0.30	1.0	5.1
NU03	55.1	0.3	0.1	35.5	0.2	0.2	7.8	b.d.l.	b.d.l.	0.6	0.03	0.1	b.d.l.	232	0.56	-2.05	0.01	0.02	0.56	9.0	3.9
NU08	48.7	0.6	0.1	40.3	0.4	0.2	9.5	0.02	b.d.l.	b.d.l.	b.d.l.	0.2	b.d.l.	508	0.49	-2.51	0.01	0.00	0.49	7.0	3.2
NU10	28.6	0.6	0.1	41.6	0.4	0.1	25.1	0.03	b.d.l.	2.5	0.08	0.7	0.05	76	0.3	-1.44	0.02	0.05	0.30	1.0	4.9
NU11	33.4	1.4	0.2	39.8	0.5	0.3	20.8	0.04	0.03	2.9	0.03	0.6	0.06	769	0.36	-1.38	0.02	0.06	0.36	2.9	4.9
NU13	50.2	1.7	0.3	37.5	0.7	0.5	7.6	0.05	0.02	1.3	b.d.l.	0.3	b.d.l.	612	0.53	-1.71	0.03	0.03	0.53	8.1	4.4
NU15	34.8	0.7	0.2	37.7	0.8	0.4	14.9	0.07	0.04	8.5	0.2	1.7	0.05	533	0.4	-0.92	0.02	0.16	0.40	4.0	5.7
NU17	27.8	2.2	0.3	35.6	1.3	0.5	19.5	0.1	0.03	9.9	0.6	2.0	0.06	4602	0.35	-0.81	0.05	0.18	0.34	2.4	5.9
NU18	37.0	0.8	0.2	41.7	0.6	0.4	15.8	0.1	0.04	2.7	0.08	0.5	0.06	445	0.39	-1.42	0.02	0.05	0.39	3.8	4.9

LA15, LA18, LA20), one sample from section NO (NO1) and three samples from section NU (NU1, NU3, NU17). In total, DNA was extracted and amplified successfully from 29 samples. These were then pooled into a single library and purified using QIAquick Gel Extraction Kit (Qiagen, Venlo, the Netherlands). The library was quantified with qPCR (KAPA Library Quantification Kits, Kapa Biosystems, Wilmington, MA, USA) and sequenced on an Illumina MiSeq using  $2 \times 300$  cycles of paired-end sequencing.

Bacterial sequences were analyzed using the USEARCH (v8.1.1861) software following the UPARSE pipeline (Edgar, 2013). After trimming to 260 bp the paired-end reads were merged and primers were removed. Merged sequences were quality filtered using maximum expected error of 0.5. Following dereplication and singleton removal, the sequences were clustered de novo into OTUs (operational taxonomic units) based on 97% similarity using the UPARSE-OTU algorithm (Edgar, 2013) which automatically detects and filters out chimeras with high efficiency. All original reads were mapped to the created non-chimeric OTUs and aligned to the SILVA database (version 132; release date 13.12.17) (Quast et al., 2013) with an identity threshold of 0.97, yielding an OTU table with a total of 5871 OTUs and 720,714 reads. Original reads are uploaded to NCBI, Sequence Read Archive (SRA) data, BioProject accession number PRJNA753265.

## 2.5. Statistical analysis

All statistical analyses have been conducted in R version 3.5. To determine the relationships between brGDGT abundances, ratios and environmental parameters, Pearson's product-moment correlations were performed using the function `cor.test`. Here, the Pearson  $r$  value and  $p$ -value are reported as measures of correlation performance, correlations with  $p$ -values  $< 0.05$  are reported as significant (Table 3). A principal component analyses was conducted to visualize: (i) the variance in the scaled fractional abundance of brGDGT lipids, and (ii) the variance in soil chemical parameters. Additional environmental parameters of interest and brGDGT ratios have been plotted a posteriori in the ordination space, using the `vegan` package (Oksanen et al., 2019).

Following the generation of the OTU table, bacterial community composition analyses were done using the packages `vegan` (Oksanen et al., 2019), `phyloseq` (McMurdie et al., 2013) and `pvcust` (Suzuki and Shimodaira, 2006). Unrarefied data represented 11,387 taxa across 29 samples. After rarefaction, the number of bacterial taxa was 4457 between all samples. One sample (NO10) has fewer sequences (942) than the rarefaction depth (9015) and was therefore discarded. To determine which soils have a similar bacterial community composition, hierarchical clustering via multiscale bootstrap resampling was performed employing the `ward.D2` agglomerative method, using bray distance (package "`pvcust`"). A bio-indicator approach was used to identify those families (taxonomic level) and OTUs that are enriched in soil clusters of interest. The function "`signassoc`" (R package `indicspecies`; De Cáceres and Legendre, 2009), computes the permutation  $p$ -value of the positive association between an OTU (or family) vector and a vector of memberships to a site-group. The approach is similar to the approach previously used in De Jonge et al. (2019; 2021) with the significant changes on family level now determined after agglomeration of the OTU count on this level.

## 3. Results

### 3.1. Environmental variables

There was a strong correlation between altitude and Mean Annual Air Temperature (MAAT range:  $-4.7$  to  $2.7$ , lapse rate:  $-0.63$  °C/100 m,  $r = -0.95$ ,  $p < 0.01$ ), as well as with Mean Annual Soil Temperature (MAST range:  $-2.5$  to  $4.3$ , lapse rate:  $-0.42$  °C/100 m,  $r = -0.80$ ,  $p < 0.01$ ). MAAT was generally lower than MAST (difference between  $-5$  °C and  $+1$  °C), possibly caused by the impact of snow insolation (Fig. 1).

**Table 3**  
Linear correlations of those lipid parameters reported in Table 2 with selected soil chemical parameters (pH, CEC, base saturation, exchangeable calcium) and temperature parameters (MAAT, MAST, MSST and GDD). The Pearson  $r$ -value and  $p$ -value are reported only for significant correlations ( $p < 0.05$ ).

	BrGDGT fractional abundance (%)												pH <sub>rec</sub>									
	Ia	Ib	Ic	IIa	IIb	IIc	IIIa	IIIb	IIIc	IIa'	IIb'	IIIa'		IIIb'	IIIc'	brGDGT ng g <sup>-1</sup> soil	MBT <sub>SME</sub>	CBT	DC'	IR	CI	MAAT <sub>rec</sub> (°C)
pH - r	-0.63						0.62	0.47							0.41	-0.60	0.47	0.46	0.46	-0.61	-0.6	0.47
pH - p	<0.01						<0.01	<0.01							<0.05	<0.01	<0.01	<0.01	<0.01	<0.01	<0.01	<0.01
Exch. Ca - r		0.46					0.54	0.39							0.51	0.38	0.38	0.62	0.52	0.62	0.38	0.38
Exch. Ca - p		<0.01					<0.01	<0.05							<0.01	<0.01	<0.01	<0.01	<0.01	<0.01	<0.05	<0.05
Base satur. - r	-0.33						0.55	0.40							0.55	0.45	0.45	0.43	0.53	0.43	0.45	0.45
Base satur. - p	<0.05						<0.01	<0.05							<0.01	<0.01	<0.01	<0.01	<0.01	<0.01	<0.01	<0.01
CEC - r																0.84	0.32	0.32	0.32		0.32	0.32
CEC - p																<0.01	0.05	0.05	0.05		0.05	0.05
MAAT - r	0.47						-0.43									0.47	0.47	0.47	0.47	0.47	0.47	0.47
MAAT - p	<0.01						<0.01									<0.01	<0.01	<0.01	<0.01	<0.01	<0.01	<0.01
MAST - r																0.32	0.32	0.32	0.32	0.32	0.32	0.32
MAST - p																0.05	0.05	0.05	0.05	0.05	0.05	0.05
MSST - r	0.43						-0.41	-0.35								0.44	0.44	0.44	0.44	0.44	0.44	0.44
MSST - p	<0.01						<0.05	<0.05								<0.01	<0.01	<0.01	<0.01	<0.01	<0.01	<0.01
GDD - r	0.43						-0.43	-0.33								0.44	0.44	0.44	0.44	0.44	0.44	0.44
GDD - p	<0.01						<0.01	<0.05								<0.01	<0.01	<0.01	<0.01	<0.01	<0.01	<0.01

Growing Degree Days (GDD range: 280–1678 °C) and the Mean Summer Soil Temperature (MSST range: 4.0–12.6 °C) both correlated well with elevation ( $r = -0.78, p < 0.01$  and  $r = -0.81, p < 0.01$ ). The temperature parameters are reported in Table 1.

Although the study region had a limited range in pH values (3.3–5.7), variability in soil chemistry was present (Supplementary Table S1). There is no significant correlation between MAAT, MAST, MSST and soil pH, and only a weak negative correlation between GDD and soil pH ( $p < 0.05, r = -0.33$ ). With the exception of exchangeable Na correlating with MSST and GDD ( $0.34 < r < 0.37, p < 0.05$ ), there is generally no correlation between the temperature parameters and the concentration of exchangeable cations (Ca, K, Mg, Na, Al, Fe, Mn (Supplementary Table S1)). The total amount of nutrients K, Mg and Na however did decrease with increasing temperatures ( $-0.69 < r < -0.53$  with MAST,  $p < 0.05$  (Supplementary Table S1)), while total Ca increased with increasing MAST ( $r = 0.34, p < 0.05$  (Supplementary Table S1)). Total P, K, Mg and Na correlate significantly with elevation ( $0.38 < r < 0.64, p < 0.05$ ). K, Mg and Na concentrations differed significantly between different transects (Transect ID = NO, NU, SO, RO and LA; Analysis of variance, Supplementary Table S2).

A principal component analysis (Supplementary Fig. S2) indicated that the main variability in soil chemistry (summed variance explained by the first 2 PCs = 54%) is effectively captured by the CEC, soil pH and base saturation. As exchangeable calcium was identified as having a strong impact on brGDGTs concentration (De Jonge et al., 2021), these four parameters (CEC, soil pH, base saturation and exchangeable calcium) will be included when discussing the impact of soil chemistry on brGDGTs and their producers.

### 3.2. Branched GDGT lipids

Thirteen brGDGTs were present in all analyzed soils, with brGDGTs IIc' and IIIc' under the quantification limit in all samples. Table 2 shows the total concentration per gram soil (between 80 and 6800 ng g<sup>-1</sup> soil) and the fractional abundance of brGDGT lipids in each soil sample. No significant correlations between the temperature parameters MAAT, MAST, MSST and GDD and the summed brGDGTs concentrations was found (Table 3). Only a non-significant positive correlation between MSST and the concentrations of brGDGT Ia and Ic was found ( $0.25 < r < 0.27, 0.10 < p < 0.12$ ; Supplementary Fig. S3). Summed concentrations of all brGDGTs correlated positively with exchangeable calcium and CEC values ( $r = 0.64$  and  $0.84$ , respectively,  $p < 0.01$ ), but did not correlate with soil pH (Table 3, Fig. 2A) or base saturation (Table 3).

The concentration of individual brGDGT compounds show positive linear correlations with CEC (CEC driven by the increase of H<sup>+</sup> ions ( $r = 0.95, p < 0.01$ )) and with exchangeable calcium (significant correlations reported in Supplementary Fig. S3). In particular, brGDGT Ia, Ic, IIa and IIc show a strong linear increase with CEC ( $0.63 < r < 0.82$ ) compared to exchangeable calcium ( $0.42 < r < 0.74$ , Supplementary Fig. S3). BrGDGTs IIIa, IIIb, IIIc, IIa', IIb', IIIa' and IIIb' show a strong linear increase with exchangeable calcium ( $0.70 < r < 0.89$ ), compared to CEC values ( $0.42 < r < 0.56$ ). BrGDGT Ib and IIb show similar correlations with CEC and exchangeable calcium ( $0.57 < r < 0.73$ ). Soils with a high concentration of exchangeable calcium generally have high base saturation values, resulting in good correlations between base saturation and the concentration of several brGDGTs (Supplementary Fig. S3).

Changes in the concentration of brGDGT lipids are reflected in the fractional abundance of these compounds at each site (Table 2). BrGDGTs Ia and IIa were the most prevalent compounds, with a fractional abundance ranging from 28% to 68% and 26% to 47%, respectively. Correlations between brGDGT lipid fractional abundances and environmental parameters (CEC, soil pH, base saturation and exchangeable calcium and temperature parameters) were calculated to identify driving factors (selected parameters reported in Table 3; Fig. 3A–C). To summarize the variation in the brGDGTs compounds, and its dependency on the environmental parameters, a principal component

analysis was performed. Fig. 2D shows the loadings of all soil samples and the individual brGDGT compounds on the first two principal components. The environmental parameters MAAT, MAST, MSST and GDD, as well as soil pH, CEC, exchangeable calcium and base saturation are plotted *a posteriori* in the ordination space (Fig. 2E). These plots show that the variation along PC1 (explains 39.1% of all variation) correlates strongly with pH ( $r = 0.61, p < 0.001$ ), available calcium ( $r = 0.39, p < 0.05$ ) as well as mean annual air temperature ( $r = -0.40, p < 0.05$ ). The variation along PC2 (which explains 20.3% of all variation) correlates with available calcium ( $r = 0.52, p < 0.01$ ), CEC ( $r = 0.35, p < 0.05$ ) and base saturation ( $r = 0.34, p < 0.05$ , Fig. 2E). Finally, PC3 explains 10.1% of the variation, and cyclopentane-containing brGDGTs Ic and Ib have a high loading, contrasted with the penta- and hexamethylated brGDGTs IIb, IIc and IIIb and IIIc (Fig. 2F). This PC correlates primarily with MSST and GDD (Fig. 2G).

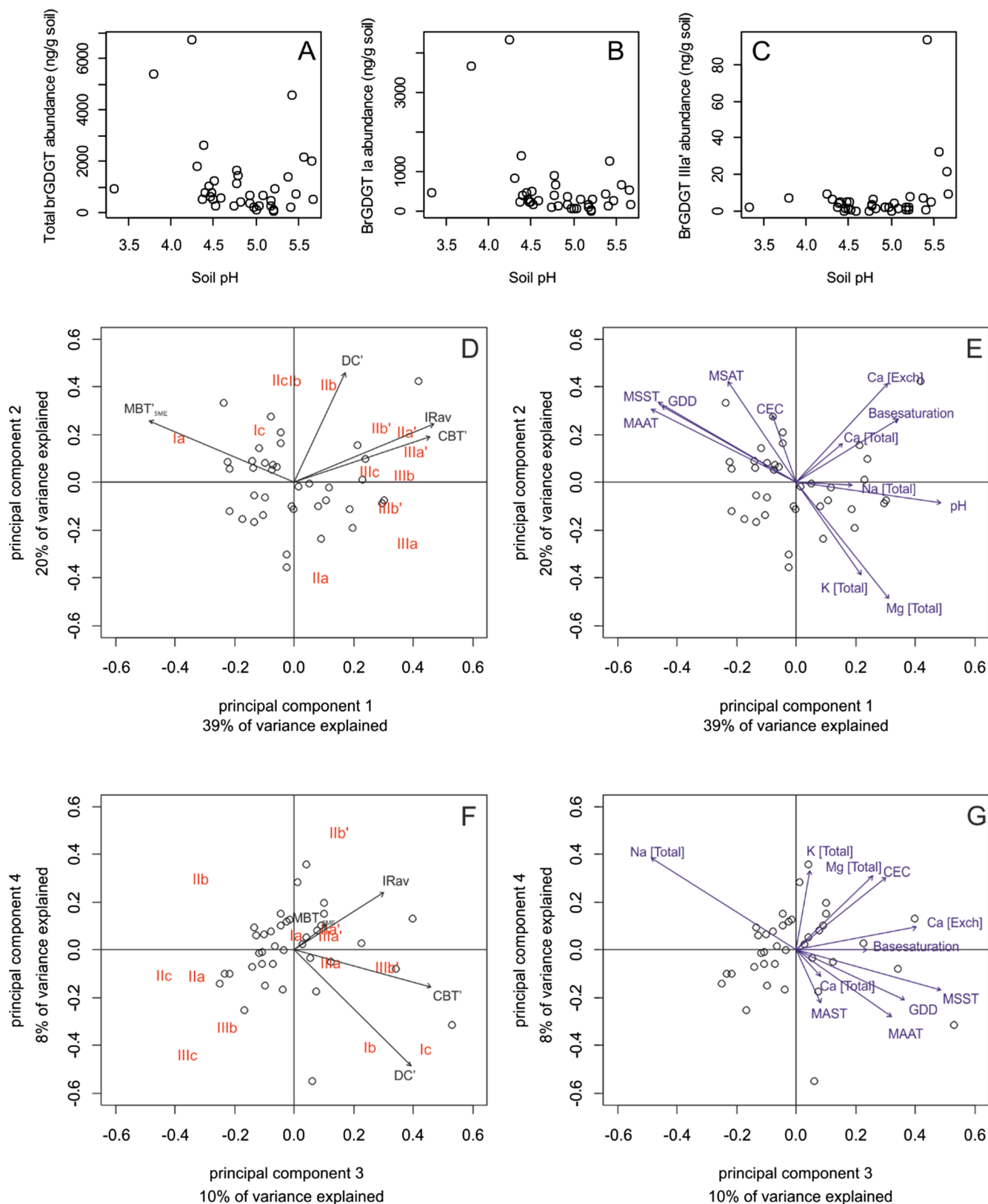
The brGDGTs distribution is further summarized using the MBT<sub>5ME</sub> and CBT' ratios (Fig. 3D, E). The MBT<sub>5ME</sub> correlates with the different temperature parameters ( $0.32 < r < 0.47, p < 0.05$ ), but shows a stronger negative correlation with soil pH ( $r = -0.60, p < 0.01$ , Fig. 3D). The CBT' ratio correlates positively with soil pH, exchangeable Ca and the base saturation ( $0.38 < r < 0.47, p < 0.05$ ), and does not correlate with temperature parameters (Table 3, Fig. 3E). The range in MBT<sub>5ME</sub> (0.30–0.70) and CBT' (-2.8 to -0.8) values result in a wide range of reconstructed temperatures (0.9–13.1 °C) and pH (2.7–5.9) values (Table 2). These reconstructed values generally overestimate measured MAST and MAAT temperatures, (residual errors range between -2 °C and 12 °C and 2 °C to 16 °C, respectively), and generally underestimate MSST (offsets from -8 °C to 5 °C). Significant correlations between brGDGT ratios and temperature and soil chemistry parameters are reported in Table 3 and plotted in Supplementary Fig. S4. Supplementary Table S3 reports an analysis of variance of the model MBT<sub>5ME</sub> ~ pH + MAAT.

### 3.3. Bacterial community composition

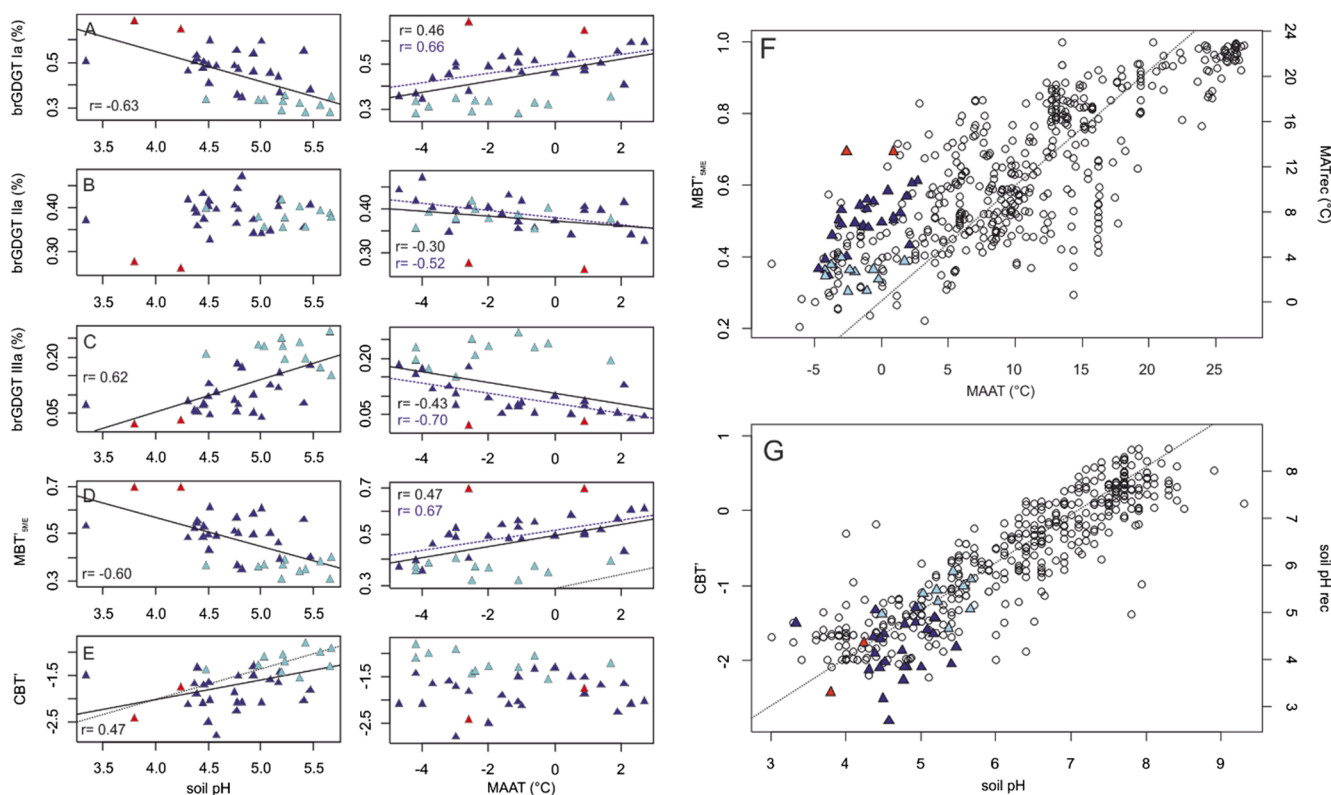
Across 28 samples, the most abundant bacterial phyla are Proteobacteria (27% of all OTU counts), Actinobacteria (25% of all OTU counts), Acidobacteria (16% of all OTU counts) and Chloroflexi (15% of all OTU counts). The most abundant 10% of all sequences are represented by just 7 OTUs from the phyla Chloroflexi (3), Proteobacteria (1) and Actinobacteria (3). Using a clustering approach, similarities in the bacterial community composition are visualized in Fig. 4A. The strong impact of pH is reflected in the distinctive pH range in both clusters: within cluster 1 soil pH ranged from 3.3 to 5.0 (Fig. 4B), while cluster 2 contains soils with generally increased pH values (4.5–5.7). The significant difference between both pH ranges is confirmed by a student *t*-test ( $p < 0.01$ ), while other soil chemical parameters (Exch. Ca, CEC, base saturation) are not statistically different between clusters.

Fig. 4C shows that cluster 1 has a higher average MAST value (2.4 °C), compared to cluster 2 (1 °C), although the average is not significantly different for either MAAT or MAST (student *t*-test). MSST and GDD ranges in cluster 1 and 2 (group mean = 9.7 and 8.1, group mean = 1154 and 855, respectively) are significantly different (student *t*-test,  $p < 0.05$ ). Cluster 2 contains a subcluster (cluster 2a,  $p = 0.81$ ; Fig. 4A), that contains those soils ( $n = 5$ ) where IR values are > 0.085 (upper 50% of range of IR values), and one soil (LA 12) with increased 6-methyl brGDGTs concentrations. Unfortunately, DNA was not successfully extracted from the high pH soil with the highest concentration of exchangeable calcium and the highest abundance of alkalinity-promoted compounds (NU17), so all bacterial community analyses are based on soils with only moderately increased IR values ( $0.085 < IR < 0.16$ ).

By identifying the families that are significantly more abundant in each bacterial cluster, a set of indicator families can be determined. We focus on Acidobacterial bio-indicators in Fig. 5 and report bio-indicator families of other phyla in Supplementary Table S4. Acidobacterial



**Fig. 2.** BrGDGT concentrations versus soil pH values ( $\text{ng}\cdot\text{g}^{-1}$  soil): (A–C) and principal component (PC) analysis based on the fractional abundances of 13 brGDGTs (D–G). (A) summed concentration of brGDGTs, (B) concentration of brGDGT Ia, (C) concentration of brGDGT IIIa', (D and F) site and species (brGDGT) loadings plotted, D plots PC1 and 2, F plots PC 3 and 4. BrGDGT ratios  $\text{MBT}_{\text{SME}}$ , CBT', DC' and IR plotted a posteriori. (E and G) soil chemical parameters and temperature parameters plotted a posteriori in the ordination space of D and F, respectively.



**Fig. 3.** Fractional abundances of brGDGT Ia, IIa and IIIa (A–C) and brGDGT based ratios  $MBT'_{SME}$  and  $CBT'$  (D–G) plotted versus soil pH and MAAT. Soils with  $CI > 0.64$  are plotted in red, soil Type 1 soils in light blue and soil Type 2 soils in dark blue. Significant linear correlations ( $p < 0.05$ ) are plotted (complete dataset: black full line, soil Type 2: dark blue dotted line, Pearson  $r$ -values reported). Panels F and G compare  $MBT'_{SME}$  and  $CBT'$  values determined in this study, within the values calculated from a dataset of globally distributed soils. Both brGDGT ratios as reconstructed MAAT and pH values (following Eqs. (5) and (6)) are plotted. In panels D, E, F and G, the calibration line between brGDGT ratios and environmental variables MAAT and pH is plotted with a black dotted line.

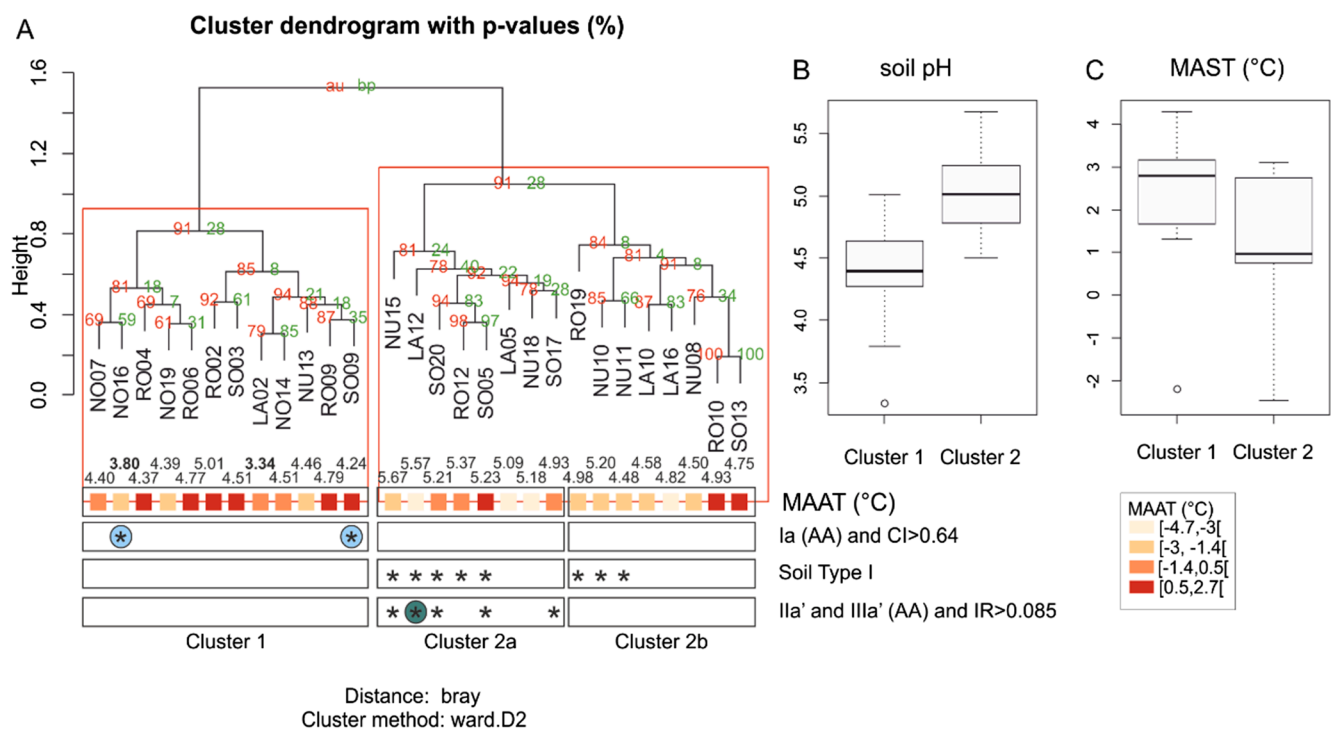


**Fig. 4.** Bacterial community composition variability: (A) depicts the cluster dendrogram, using a Bray cluster analysis, amended with information about pH, mean annual air temperature (MAAT), concentration of brGDGTs Ia, IIa' and IIIa' (absolute abundance: AA) and ratio values (CI, Ia/IIa and IR). Here, a colored circle indicates an increased concentration, and an asterisk indicates that the ratio values exceed the threshold indicated. (B and C) Boxplot of pH and mean annual soil temperature (MAST) ranges in cluster 1 and cluster 2.

subgroups 1, 3 and 12 are significantly increased in cluster 1 soils, while subgroups 6 and 7 are significantly increased in cluster 2 soils. Within cluster 2a soils, Acidobacteria subgroup 7, subgroup 10 (family ABS-19), subgroup 4, subgroup 6, subgroup 17 and subgroup 22 are significantly increased ( $p < 0.05$ ). Soils with CI values  $> 0.64$  have also been subjected to a separate bio-indicator analysis, in these soils ( $n = 2$ ) Acidobacterial subgroups 1 and 3 are significantly increased (Fig. 5, Supplementary Table S4).

## 4. Discussion

### 4.1. Environmental drivers on brGDGT proxies, concentration and distribution.

#### 4.1.1. Performance of temperature proxies and environmental dependency of brGDGTs Ia, IIa, IIIa.

The large variability in the  $MBT_{5ME}$  values, and the poor correlation with temperature parameters, result in reconstructed air temperatures ( $1\text{ }^{\circ}\text{C}$  to  $13\text{ }^{\circ}\text{C}$ ) that are distinct from measured air temperatures. Reconstructed temperatures are between  $2\text{ }^{\circ}\text{C}$  and  $16\text{ }^{\circ}\text{C}$  warmer than MAAT (Fig. 3F), which is a significantly larger offset than what is expected based on the current calibration errors ( $RSME = 4.6\text{ }^{\circ}\text{C}$ , De Jonge et al., 2014a). The offset between air and soil temperature has been proposed to be the cause of the remaining error in even the most recent calibrations (Dearing-Crampton Flood et al., 2020). However, when we use the soil temperature values collected over 1 year, the linear correlation with  $MBT_{5ME}$  values becomes worse (Table 3), and a large offset (between  $-2\text{ }^{\circ}\text{C}$  and  $12\text{ }^{\circ}\text{C}$ ) remains (Fig. 3F).

For high altitude sites, reduced production of lipids in frozen soil conditions has been proposed (Dearing Crampton-Flood et al., 2020). The MSST and GDD values summarize summer soil temperature and accumulated heat in non-frozen soil conditions, respectively. The  $MBT_{5ME}$  values still show a poor correlation with these seasonal temperature parameters ( $r = 0.44$  and  $0.44$ , respectively,  $p < 0.01$ ). While the average of the reconstructed temperatures falls close to the average MSST ( $6.1\text{ }^{\circ}\text{C}$  and  $8.5\text{ }^{\circ}\text{C}$ , respectively), the large spread in reconstructed temperatures results in offsets between  $-8\text{ }^{\circ}\text{C}$  and  $5\text{ }^{\circ}\text{C}$ , compared to measured MSST values. The additional variation in the correlation between the  $MBT_{5ME}$  values and soil temperature could be due to the short measurement period available (1 year). As brGDGTs reflect an

integrated signal over several decades, long-term averaged atmospheric temperatures reflect this better than a 1-year soil temperature record, as soil temperature spatial patterns vary between years at this site (Lembrechts et al., 2019). Ideally, brGDGT distributions should be compared with long-term soil temperature data, which could improve the observed correlations with soil temperature parameters.

Currently, the  $MBT_{5ME}$  values show a better linear correlation with soil pH ( $r = -0.60$ ,  $p < 0.01$ ), compared to temperature. The poor correlation between the  $MBT_{5ME}$  and temperature parameters (Table 3), is thus possibly caused by the strong impact of soil chemistry on the compounds that are the backbone of the  $MBT_{5ME}$  ratio. As the  $MBT_{5ME}$  values in this dataset are correlated strongly with the values of the ratio  $Ia/(Ia + IIa + IIIa)$  ( $r > 0.99$ ,  $p < 0.001$ ), the fractional abundance of brGDGTs Ia, IIa and IIIa determine the variation in the  $MBT_{5ME}$  ratio. An increase in brGDGT Ia, compared to the values of IIa and IIIa (expressed as the Community Index), was observed by De Jonge et al. (2019) to be coeval with a change in bacterial community composition. To extrapolate the lipid signal to the global scale, a threshold value of the CI index ratio was previously determined ( $CI > 0.64$ ), above which the brGDGT distribution reflected the changed bacterial community (De Jonge et al., 2019). Along the altitudinal gradient under study, 2 soils have CI values ( $CI = 0.69$ ) that fall above the threshold value. Although these soils have the highest  $MBT_{5ME}$  values ( $MBT_{5ME} > 0.65$ ), they are not the warmest soils (Fig. 3, MSST between  $1\text{ }^{\circ}\text{C}$  and  $3\text{ }^{\circ}\text{C}$ ; Supplementary Fig. S4). Instead, they are the sites with the highest brGDGT concentrations ( $\text{ng}\cdot\text{g}^{-1}$  soil) and CEC values.

The total CEC or perhaps even a direct measurement of hydrogen ion concentrations (“free acidity”) seems to explain concentration changes in main brGDGTs Ia and IIa better than soil pH (Supplementary Fig. S3). This can be because of a collapse of the brGDGT producing community in the extremely acid soils ( $\text{pH} = 3.3$ ), or a more direct effect of hydrogen ion concentrations on brGDGTs, compared to the pH values. Those soils with CEC values  $> 40$ , have large concentrations of  $\text{H}^+$  ( $30\text{--}60\text{ meq}\cdot 100\text{ g}^{-1}$  soil), and only intermediate concentrations of exchangeable Ca ( $5\text{--}8\text{ meq}\cdot 100\text{ g}^{-1}$  soil).

A possible explanation for this soil chemistry could be very slow decomposition and allelopathic root systems in a system often dominated by *Empetrum nigrum* ssp. *hermaphroditum* (Tybirk et al., 2000). In addition, because of the limited soil depth and the often steep slopes, water availability can fluctuate throughout the season (e.g., Crave and

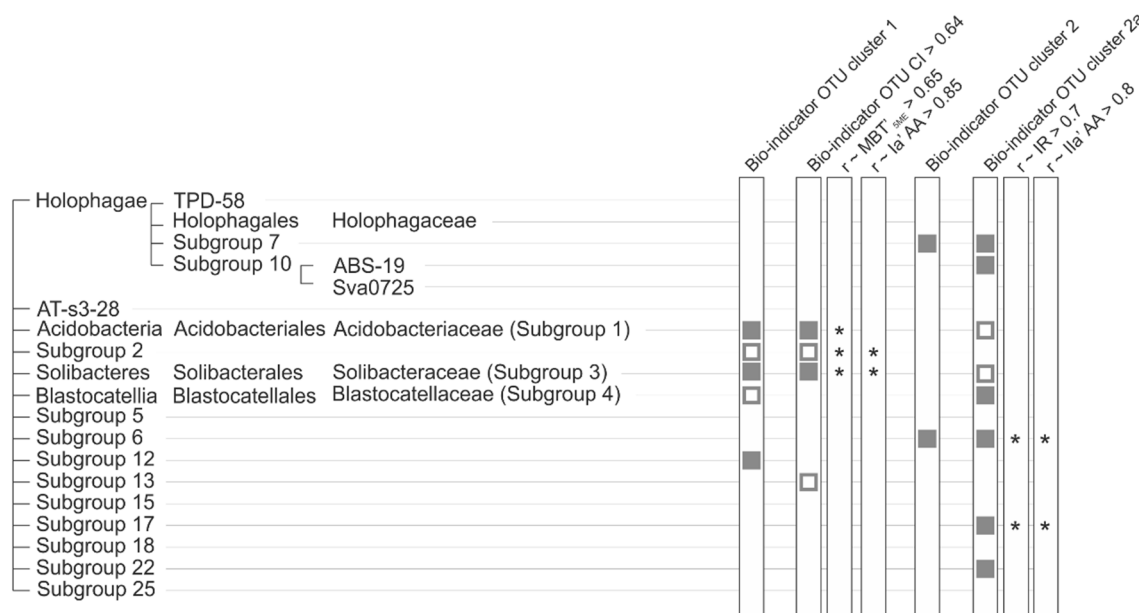


Fig. 5. Distribution of bio-indicator OTUs (empty squares) and bio-indicator families (full squares) in cluster 1, high CI soils, cluster 2 and cluster 2a soils. Asterisks indicate which clades contain bio-indicator OTU that show the strongest correlation (based on Pearson r-values) with brGDGT ratios and brGDGT concentrations.

Gascuel-Oudou, 1997; Moore et al., 1988), affecting the concentration of hydrogen ions in the soils. The absence of a temperature threshold for  $CI > 0.64$  soils along the altitudinal gradient is expected based on the global scale, where no temperature cut-off was present between “typically cold” and “typically warm” soils (De Jonge et al., 2019).

As high  $CI$  values along a geothermal gradient were observed to occur only when the bacterial community changes, we now evaluate whether this holds true in the altitudinal  $CI > 0.64$  soils. Several bio-indicator OTUs and families were detected in these soils (Fig. 5, Supplementary Table S4). Focusing on Acidobacterial diversity, an increase in subgroups 1 and 3 was observed. This increase is shared with the high  $CI$  soils ( $>0.64$ ) encountered along the geothermal gradient (De Jonge et al., 2019). The rarefied (i.e., fractional) abundance of a subset of OTUs in subgroups 1, 2 and 3 correlate with  $MBT'_{5ME}$  values in soils ( $r > 0.65$ ,  $p < 0.01$ ), and with the concentration of brGDGT Ia in soils ( $r > 0.8$ ,  $p < 0.05$ ). We propose that a change in the composition of the bacterial community can be the cause of the increased  $CI$  values ( $>0.64$ ) in the high CEC altitudinal soils. As the fractional abundance of brGDGTs Ia, IIa and IIIa matches the global distribution (Supplementary Fig. S5A,B), soil chemistry (specifically, CEC or free acidity), modulating bacterial community composition, can thus play a role in generating high  $CI$  values in Typically Warm soils on a global scale.

Also in the other soils ( $CI < 0.64$ ), pH plays a strong role in the distributions of brGDGTs Ia, IIa and IIIa (Fig. 3). In the absence of a temperature signal, an increase in alkalinity-promoted compounds is expected to decrease the fractional abundance of these three main brGDGTs (De Jonge et al., 2021). Along the altitudinal gradient, we observed a decrease in the fractional abundance of brGDGT Ia ( $r = -0.63$ ,  $p < 0.05$ ) and an increase in the fractional abundance of brGDGT IIIa ( $r = 0.62$ ,  $p < 0.05$ ) with pH, caused by changes in their concentration (Supplementary Fig. S3). A stepwise pattern can be recognized, with a decreased percentage of brGDGT Ia in a group of high pH soils (Fig. 3A, light blue symbols), where IIIa is increased (Fig. 3C, light blue symbols). In the diagnostic scatterplot between brGDGT Ia and IIa, this decrease in brGDGT Ia is visible as an offset from the negative correlation between brGDGT Ia and IIa (Fig. 6A, light blue symbols). This group

of generally high pH soils (pH 4.4–5.7) is referred to as “Type 1 soils” in the further discussion. The remaining soils (referred to as “Type 2 soils”) fall in the low pH bracket (pH 3.3–5.4).

Importantly, pH values do not allow us to distinguish between these soils, as there is an overlap in pH values (Fig. 3A–C). Also, there is no difference in MAAT values between Type 1 and Type 2 soils (Fig. 3A–C and 6B). Type 1 and Type 2 soils show a change in brGDGT signature, and a different environmental dependency that affects the  $MBT'_{5ME}$  values and causes the pH dependency. Specifically, soils of similar MAAT values have different fractional abundances of brGDGT Ia and IIIa (Fig. 3A, 3C and 6B). Furthermore, in Type 2 soils, strong significant correlations between the main brGDGTs Ia, IIa and IIIa fractional abundance and MAT are observed ( $|0.30| < r < |0.46|$ ,  $p < 0.01$ ), that are absent in the Type I soils (Fig. 3). Although there is no clear threshold in soil pH between Type 1 and Type 2 soils, they show a different pH range (Fig. 3). Previously, pH-dependent changes in the brGDGT dependencies have been shown to be related to changes in the bacterial community composition. Below, we evaluate in more detail through which mechanisms pH, and other parameters of soil chemistry, influence the production of brGDGTs.

#### 4.1.2. Performance of pH proxies and environmental dependence of alkalinity-promoted compounds

In the soils under study, soil pH (3.3–5.7) had a compounded effect on the concentration of all brGDGTs. Increased concentrations of brGDGTs at intermediate pH (pH 3.8 and 4.2) are caused by an increase in brGDGTs Ia, Ib, Ic, IIa, IIb, IIc, IIIb and IIIc (Supplementary Fig. S3). The brGDGTs IIa, IIb, IIc, IIIa, IIIb and IIIc show a second maximum at relatively high pH values (pH  $> 5.4$ ). 6-Methyl brGDGTs on the other hand increase only above the pH threshold of 5.5. The complex and non-linear behavior of brGDGT concentration along the pH gradient can be explained by a composition of linear dependencies of brGDGTs on different soil cations. Firstly, high soil CEC (driven mainly by the variation in exchangeable  $H^+$  ions) correlates best with the concentrations of the 5-methyl brGDGTs Ia, Ic, IIa and IIc. As a second driver of brGDGT concentrations, exchangeable calcium concentrations show strong

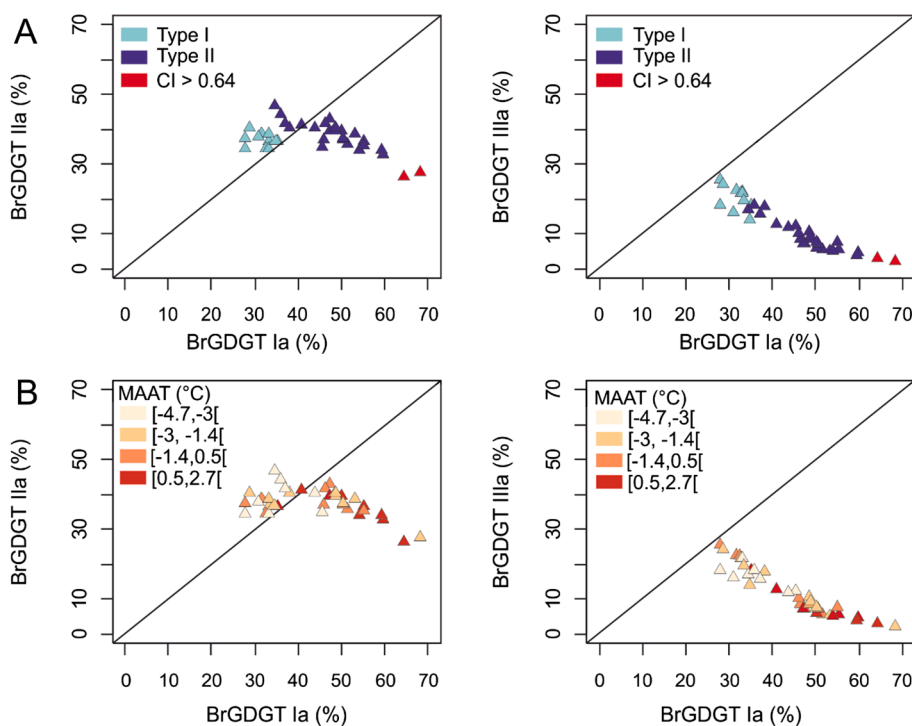


Fig. 6. Fractional abundances (%) of major brGDGTs Ia, IIa and IIIa, with symbol colors reflecting Type 1, Type 2 and Cluster Warm soils (A) and mean annual air temperature (MAAT; B).

linear correlations with the concentration of hexamethylated brGDGTs (IIIa, IIIb, IIIc) and 6-methyl brGDGTs (IIa', IIb', IIIa', IIIb' (Supplementary Fig. S3)).

The strong impact of pH, CEC and exchangeable calcium on the brGDGT concentrations is mirrored in the impact on the fractional abundances of alkalinity-promoted compounds (cyclopentane containing compounds and 6-methyl compounds) and the pH proxies CBT', DC' and IR (Table 3, Fig. 2E). Specifically, the previously observed pH-dependency of the fractional abundance of 6-methyl brGDGTs is supported. However, with the exception of brGDGT IIIb, the fractional abundances of brGDGTs with 1 cyclopentane group (Ib, IIb and IIb') do not show a linear dependency on pH. Several ratios have been developed that reflect soil pH on a global scale. Of these, the IR of hexamethylated compounds (IR<sub>IIIa</sub>) shows no significant correlation with pH, as both IIIa and IIIa' increase in fractional abundance with pH. The IR ratio of pentamethylated compounds (IR<sub>IIa</sub>) and the IR (which uses both IIa and IIIa) however, do correlate with soil pH ( $r = 0.48$  and  $r = 0.46$ , respectively,  $p < 0.01$ ). Instead of pH, exchangeable calcium seems a better predictor of the fractional abundance of alkalinity-promoted compounds along the altitudinal gradient. The 6-methyl brGDGTs (IIa', IIb', IIIa') as well as the cyclopentane-containing brGDGTs (Ib, IIb, IIIb) show a calcium-dependent increase in fractional abundance (Table 3). This results in a significantly better correlation between DC' and exchangeable calcium, compared to soil pH. The CBT' and IR ratio, show a similar or slightly weaker correlation with exchangeable calcium, compared to soil pH. What is generally assumed to be a homogeneous group of alkalinity-promoted ratios (IR<sub>IIa</sub>, IR<sub>IIIa</sub>, DC', CBT'), thus seem to respond to different parameters in this pH range (pH 3.3–5.7). The concentration of exchangeable calcium (in addition to soil pH) was previously identified as being a possible driving factor behind changes in alkalinity-promoted brGDGT concentrations across large pH gradients (4.5–7.5, De Jonge et al., 2021). The impact of exchangeable calcium on brGDGTs concentration and fractional abundance in the lower pH bracket under study, supports that calcium impacts brGDGT concentrations and distribution. We propose that the availability of calcium is relevant for the response of alkalinity-promoted compounds and pH proxies across the globe (De Jonge et al., 2014a; Duan et al., 2020; De Jonge et al., 2021).

Previously, De Jonge et al. (2021) attributed a pH-dependent change in brGDGT lipids to a change in bacterial community composition. Along our altitudinal gradients, soil pH again explains the largest part of the variation in the bacterial community composition (Fig. 4A, B). Cluster 1 contains low pH soils (3.3–5.0), while higher pH soils (4.5–5.7, including Type 1 soils) fall in cluster 2. Soils with increased amounts of 6-methyl brGDGTs fall specifically in cluster 2a (Fig. 4B). Cluster 1, which also contains the high CI soils, shows an increase in Acidobacterial subgroups 1, 3 and 12. A significant increase in Acidobacterial subgroups 6 and 7 is observed within cluster 2 and 2a soils. The diversity of Acidobacterial subgroups that is increased in the cluster 2a specifically is larger, with subgroups 4, 10, 17 and subgroup 22 increased in addition to subgroup 6 and 7 (Fig. 5). Previous environmental studies found that soils with increased pH values (pH ~ 6.1, Iceland, Scotland, The Netherlands (De Jonge et al., 2021)), showed an increase in OTUs from Acidobacteria subgroup 6. Soils within cluster 2 and 2a are thus characterized by a similar change in bacterial community composition. These soils are encountered at a slightly lower pH values (4.9–5.7) than previously observed thresholds and can be interpreted as the lower range at which the production of 6-methyl brGDGTs is encountered. Remarkably, not all soils within clusters 2 and 2a show increased amounts of brGDGT IIIa and 6-methyl brGDGTs. Instead, this increase is present only in the soils that have moderately (brGDGT IIIa) or strongly (6-methyl brGDGTs) increased concentrations of exchangeable calcium (Supplementary Fig. S3). This could reflect a mechanism where calcium has a direct impact on production of brGDGT IIIa and 6-methyl brGDGTs in the bacterial cell membrane. Alternatively, calcium can promote the increase in 6-methyl producing bacterial lineages. This

is supported by the observation that the rarefied abundance (the rarefied OTU count represents the fractional abundance compared with a total of 9015 counts) of certain OTUs placed within Acidobacterial subgroup 6 and subgroup 17 correlate with the concentration of brGDGT IIa' ( $r > 0.8$ ,  $p < 0.01$ ), and the IR values ( $r > 0.7$ ,  $p < 0.01$ ) in the soils (Fig. 5). This may indicate that an increase in the importance of OTUs placed within Acidobacterial subgroup 6 and 17 directly relates to an increase in 6-methyl brGDGTs in soils.

#### 4.2. Implications for the interpretation of the MBT<sub>5ME</sub> paleotemperature proxy

The range in MBT<sub>5ME</sub> values encountered at this site represents a large fraction of the range in MBT<sub>5ME</sub> values present on the global scale (49%, Fig. 3F). Firstly, we propose that the variation in MBT<sub>5ME</sub> values is caused by the interplay between a changed composition of their bacterial producers, and the direct impact of soil chemical parameters. Soils with CI values  $> 0.64$ , have MBT<sub>5ME</sub> values that exceed the expected value based on the global calibration (Supplementary Fig. S5C), and cause a large part of the offset between reconstructed and measured MAAT values (offset of 12.5 °C and 16 °C). The high CEC values in high CI soils (part of cluster 1 soils), possibly promote the Acidobacterial subgroups 1 and 3 that are present within cluster 1 soils (Fig. 5). Secondly, a change in brGDGT fingerprint between Type 1 and Type 2 soils, causes the MBT<sub>5ME</sub> values to vary with soil pH, where Type 1 soils have decreased MBT<sub>5ME</sub> values, and type 2 soils show a better correlation with MAAT ( $r = 0.67$ , compared to  $r = 0.47$  for the complete dataset; Fig. 3). Although Type 1 soils all fall within bacterial community cluster 2 (Fig. 4), not all cluster 2 soils follow the Type 1 soil pattern, which have an offset MBT<sub>5ME</sub> value. Not separated by any of the environmental parameters under study (although mean pH values are significantly different,  $t$ -test  $p < 0.01$ ), an unknown environmental factor might determine the production of a Type 1 lipid signature in soils with a bacterial community typical for cluster 2 soils. Alternatively, this imperfect fit between bacterial community composition and brGDGT distribution can be caused by a temporal offset between the long-lived lipid pool and a more recent bacterial DNA signature. In this study, an analysis of variance shows that soil pH explains 36% of variation in the MBT<sub>5ME</sub>, with MAAT explaining only an additional 11% (Supplementary Table S3). However, this percentage will differ depending on the range of temperature and pH values within each dataset.

The altitudinal gradient under study thus illustrates how bacterial community changes, driven by soil chemistry changes, impact the MBT<sub>5ME</sub> values. As soil chemistry determines the bacterial community composition, this causes the MBT<sub>5ME</sub> values to show a better correlation with soil chemistry parameters pH, total Mg and total P ( $-0.60 < r < -0.54$ ,  $p < 0.01$ ) than with temperature parameters ( $0.44 < r < 0.47$ , with MAAT and MST: Table 3, Supplementary Fig. S4). As soil chemistry parameters show a dependency on altitude and/or temperature in our study region, we evaluate whether the remaining correlation with temperature parameters is possibly an indirect ("secondary") effect. The total amount of Ca increased with increasing MAST ( $r = 0.34$ ,  $p < 0.05$ ), while total amount of nutrients K, Mg and Na decrease with increasing MAST ( $-0.69 < r < -0.53$ ,  $p < 0.05$ ). This elevation and/or temperature-dependent soil chemistry can be caused by several factors. Firstly, an underlying change in local bedrock geology possibly contributes to the elevation and temperature correlation of total K, Mg and Na (Supplementary Table S2). Secondly, a dependency between soil chemistry and elevation can be caused by downslope transport of water and nutrients (Seibert et al., 2007). Thirdly, the positive correlation between MAST and total Ca can be caused by the more extensive development of soils at warmer, lower-elevation sites, which represents a direct link between soil chemistry and temperature. The exchangeable cation concentrations and pH, that had a more direct impact on brGDGT concentrations, don't show a significant correlation with elevation and/or temperature on the spatial scale under study. On larger spatial scales however, pH as well as

exchangeable cations (Al, Ca, K, Mg, Na) do vary significantly with elevation in Swedish soils (Seibert et al., 2007). Elevation and/or temperature correlate with larger scale patterns in soil chemistry, while small-scale topography, influencing vegetation type and uptake possibly drive variation in concentration of exchangeable cations along our altitudinal gradients.

The dependency between soil chemistry (pH is often the reported parameter) and altitude holds true for several altitudinal transects that have been used to determine the temperature dependency of brGDGT lipids. For instance, Peterse et al. (2009), Coffinet et al. (2014) and Véquaud et al. (2021) report that altitude and pH show a negative correlation (pH range 5.5–7.3,  $r = -0.48$ ,  $p = 0.02$  (African Mt. Rungwe), pH range 4.4–7.9,  $r = -0.67$ ,  $p < 0.01$  (Chinese Mt. Gongga), pH range 3.6–7.5,  $r = -0.44$  (French Alps)). Wang et al. (2018) report positive correlations between soil pH and altitude (pH range 3.5–6.0,  $r^2 = 0.68$  (Chinese Mt. Fanjing), pH range 5–6.5,  $r^2 = 0.63$  (Chinese Mt. Gaoligong)). On Chinese Mt. Shennongjia, the soil pH (5–8) did not vary linearly with altitude (Wang et al., 2018). Although no global dependency of the MBT<sub>5ME</sub> values on soil pH is observed (De Jonge et al., 2014a), soil pH correlates with the MBT<sub>5ME</sub> values along the altitudinal gradient under study. The correlation between soil pH and altitude in several published MBT/CBT and MBT<sub>5ME</sub> dependencies, warrants caution in interpreting these ratios as being uniquely driven by temperature. Instead, both soil chemistry and temperature are expected to influence MBT<sub>5ME</sub> values in soils collected along altitudinal gradients.

Our results raise some important considerations to keep in mind when interpreting brGDGT ratio values in geological archives. For example, this study confirms that the CI threshold value (CI = 0.63) has the potential to trace bacterial community changes that influence the MBT<sub>5ME</sub> ratio, in the absence of a temperature change. We recommend evaluating the values of this ratio, prior to interpreting the MBT<sub>5ME</sub> as a temperature proxy. Furthermore, this study shows that in soils within this low pH bracket under study (3.3–5.7), the dependency of major brGDGTs Ia and IIa can change, possibly modulated by a change in bacterial community. To recognize this in downcore GDGT distributions, the diagnostic scatterplots shown in Fig. 6 can be used. Furthermore, the CBT' can be used to reconstruct changes in soil chemistry that could have impacted the MBT<sub>5ME</sub>-temperature dependency, as these bacterial community changes resulting in a Type 1 and Type 2 brGDGT signature, reflect a different soil pH.

## 5. Conclusions

We have investigated the impact of temperature and soil chemistry on brGDGT concentrations, fractional abundances and their bacterial producers along altitudinal gradients in the northern Scandinavian Mountains. For the temperature parameters, the MBT<sub>5ME</sub> ratio only showed a significant correlation with MAAT (0.47,  $p < 0.01$ ). Using the MAST, removing the offset between air and soil temperature, did not improve the correlation. Using MSST and GDD, reconstructed temperatures showed a smaller offset with MSST, indicating that the brGDGTs along this subarctic gradient reflect summer temperatures more closely. Soils with increased concentrations of brGDGT Ia and IIa, characterized by CI > 0.64 and the highest MBT<sub>5ME</sub> values, showed a change in the composition of Acidobacterial OTUs. These soils were not present in the plots with the warmest temperatures, and we propose that a shift in bacterial community composition in these soils caused the largest offsets with measured MAAT. Soil pH was furthermore shown to act on the concentration of brGDGT IIa and IIIa, resulting in MBT<sub>5ME</sub> values that correlate best with soil pH ( $r = -0.60$ ,  $p < 0.01$ ). Similar to findings in De Jonge et al. (2021), this shift in brGDGT signature, and the potential to produce 6-methyl brGDGTs was largely coeval with a shift in bacterial community composition. The concentration of alkalinity-promoted compounds correlated better with the concentration of exchangeable calcium, which indicates a more direct effect of calcium on the brGDGT lipids, compared to soil pH. An impact of Ca<sup>2+</sup> on the distribution of

archaeal isoGDGTs lipids (Naafs et al., 2018) indicates that the effect of this soil cation is an important parameter influencing both archaeal and bacterial producers of GDGT lipids.

The variation in MBT<sub>5ME</sub> values spans a significant part of the global range in MBT<sub>5ME</sub> values. The relative importance of soil pH and temperature on the variation in MBT<sub>5ME</sub> values can be expected to depend on the temperature and pH range under study. As pH (controlling several soil chemical factors) and elevation often correlate, its impact on the temperature dependency of brGDGTs along altitudinal gradients warrants further investigation. Moving forward, we propose to measure a wider diversity of soil chemical parameters and longer-term in situ soil parameters to determine the environmental drivers of soil brGDGT lipids. To confirm the impact of bacterial community composition on brGDGT concentrations and derived ratios, a combined DNA and lipid approach should be used at diverse locations. BrGDGT-based bacterial community ratio CI, the pH dependent CBT' and the linear dependencies between brGDGT Ia, IIa and IIIa can be used to determine the impact of bacterial community changes on modern and geological brGDGT distributions.

## Declaration of Competing Interest

The authors declare that they have no known competing financial interests or personal relationships that could have appeared to influence the work reported in this paper.

## Acknowledgements

We thank Klaas Nierop and Francien Peterse for laboratory assistance at the University of Utrecht, as well as Tom Van der Spiet at the University of Antwerp. We thank Ronja Wedegärtner for help in the field. The authors gratefully acknowledge support of the Research Fund of the University of Antwerp (BOF/FFB180030). We thank the two reviewers for their constructive feedback that improved the current version of the manuscript. J.J.L. acknowledges funding from the Research Foundation Flanders (12P1819N) and a travel grant from the EU INTERACT Arctic Access program. C.D.J. acknowledges funding from ERC H2020 Marie Skłodowska-Curie Actions (grant agreement n° 707270/WISLAS).

## Appendix A. Supplementary material

Supplementary data to this article can be found online at <https://doi.org/10.1016/j.orggeochem.2021.104346>.

## References

- Brown, I.C., 1943. A rapid method of determining exchangeable hydrogen and total exchangeable bases of soils. *Soil Science* 56, 353–358.
- Caporaso, J.G., Lauber, C.L., Walters, W.A., Berg-Lyons, D., Lozupone, C.A., Turnbaugh, P.J., Fierer, N., Knight, R., 2011. Global patterns of 16S rRNA diversity at a depth of millions of sequences per sample. *Proceedings of the National Academy of Sciences* 108 (Supplement 1), 4516–4522.
- Coffinet, S., Hugué, A., Williamson, D., Fosse, C., Derenne, S., 2014. Potential of GDGTs as a temperature proxy along an altitudinal transect at Mount Rungwe (Tanzania). *Organic Geochemistry* 68, 82–89.
- Cáceres, M.D., Legendre, P., 2009. Associations between species and groups of sites: indices and statistical inference. *Ecology* 90 (12), 3566–3574.
- Crave, A., Gascuel-Oudou, C., 1997. The influence of topography on time and space distribution of soil surface water content. *Hydrological Processes* 11, 203–210.
- De Jonge, C., Hopmans, E.C., Stadnitskaia, A., Rijpstra, W.I.C., Hofland, R., Tegelaar, E., Sinninghe Damsté, J.S., 2013. Identification of novel penta- and hexamethylated branched glycerol dialkyl glycerol tetraethers in peat using HPLC-MS<sup>2</sup>, GC-MS and GC-SMB-MS. *Organic Geochemistry* 54, 78–82.
- De Jonge, C., Hopmans, E.C., Zell, C.I., Kim, J.-H., Schouten, S., Sinninghe Damsté, J.S., 2014a. Occurrence and abundance of 6-methyl branched glycerol dialkyl glycerol tetraethers in soils: implications for palaeoclimate reconstruction. *Geochimica et Cosmochimica Acta* 141, 97–112.
- De Jonge, C., Stadnitskaia, A., Hopmans, E.C., Cherkashov, G., Fedotov, A., Sinninghe Damsté, J.S., 2014b. In situ produced branched glycerol dialkyl glycerol tetraethers in suspended particulate matter from the Yenisei River, Eastern Siberia. *Geochimica et Cosmochimica Acta* 125, 476–491.

- De Jonge, C., Radujković, D., Sigurdsson, B.D., Weedon, J.T., Janssens, I., Peterse, F., 2019. Lipid biomarker temperature proxy responds to abrupt shift in the bacterial community composition in geothermally heated soils. *Organic Geochemistry* 137, 103897.
- De Jonge, C., Kuramae, E.E., Radujković, D., Weedon, J.T., Janssens, I.A., Peterse, F., 2021. The influence of soil chemistry on branched tetraether lipids in mid- and high latitude soils: Implications for brGDGT- based paleothermometry. *Geochimica et Cosmochimica Acta* 310, 95–112.
- Dearling Crampton-Flood, E., Tierney, J.E., Peterse, F., Kirkels, F.M.S.A., Sinninghe Damsté, J.S., 2020. BayMBT: a Bayesian calibration model for branched glycerol dialkyl glycerol tetraethers in soils and peats. *Geochimica et Cosmochimica Acta* 268, 142–159.
- Ding, S., Xu, Y., Wang, Y., He, Y., Hou, J., Chen, L., He, J.-S., 2015. Distribution of branched glycerol dialkyl glycerol tetraethers in surface soils of the Qinghai-Tibetan Plateau: implications of brGDGTs-based proxies in cold and dry regions. *Biogeosciences* 12, 3141–3151.
- Duan, Y., Sun, Q., Werne, J.P., Yang, H., Jia, J., Wang, L., Xie, H., Chen, F., 2020. Soil pH dominates the distributions of both 5- and 6-methyl branched tetraethers in arid regions. *Journal of Geophysical Research Biogeosciences* 125 e2019JG005356.
- Edgar, R.C., 2013. UPARSE: highly accurate OTU sequences from microbial amplicon reads. *Nature Methods* 10, 996–998.
- Haider, S., Lembrechts, J., McDougall, K., Pauchard, A., Alexander, J.M., Barros, A., Cavieres, L., Rashid, I., Rew, L., Aleksanyan, A., Sierra, J.A., Aschero, V., Chisholm, C., Clark, V.R., Clavel, J., Daehler, C., Dar, P., Dietz, H., Dimarco, R., Edwards, P., Essl, F., Fuentes-Lillo, E., Guisan, A., Gwate, O., Hargreaves, A., Jakobs, G., Jiménez, A., Kardol, P., Küffer, C., Larson, C., Lenoir, J., Lenzner, B., Mederos, M.P., Mihoc, M., Milbau, A., Morgan, J., Müllerová, J., Naylor, B., Nijs, I., Nuñez, M., Otto, R., Payne, D., Preuk, N., Backes, A.R., Reshi, Z.A., Rumpf, S., Sandoya, V., Schroder, M., Speziale, K., Valencia, G., Vandvik, V., Vítková, M., Vorstenbosch, T., Walker, T., Walsh, N., Wright, G., Zong, S., Seipel, T., 2021. Think globally, measure locally: The MIREN standardized protocol for monitoring species distributions along elevation gradients (preprint). Preprints. <https://doi.org/10.22541/au.162219027.79625324/v1>.
- Hopmans, E.C., Schouten, S., Sinninghe Damsté, J.S., 2016. The effect of improved chromatography on GDGT-based palaeoproxies. *Organic Geochemistry* 93, 1–6.
- Karger, D.N., Conrad, O., Böhner, J., Kewahl, T., Kreft, H., Soria-Auza, R.W., Zimmermann, N.E., Linder, H.P., Kessler, M., 2017. Climatologies at high resolution for the earth's land surface areas. *Scientific Data* 4 (1). <https://doi.org/10.1038/sdata.2017.122>.
- Lei, Y., Yang, H., Dang, X., Zhao, S., Xie, S., 2016. Absence of a significant bias towards summer temperature in branched tetraether-based paleothermometer at two soil sites with contrasting temperature seasonality. *Organic Geochemistry* 94, 83–94.
- Lembrechts, J.J., Pauchard, A., Lenoir, J., Nuñez, M.A., Geron, C., Ven, A., Bravo-Monasterio, P., Teneb, E., Nijs, I., Milbau, A., 2016. Disturbance is the key to plant invasions in cold environments. *Proceedings of the National Academy of Sciences* 113, 14061–14066.
- McMurdie, P.J., Holmes, S., Watson, M., 2013. phyloseq: An R Package for reproducible interactive analysis and graphics of microbiome census data. *PLOS ONE* 8, e61217. <https://doi.org/10.1371/journal.pone.0061217>.
- Lembrechts, J.J., Lenoir, J., Roth, N., Hattab, T., Milbau, A., Haider, S., Pellissier, L., Pauchard, A., Ratier Backes, A., Dimarco, R.D., Nuñez, M.A., Aalto, J., Nijs, I., Bates, A., 2019. Comparing temperature data sources for use in species distribution models: from in-situ logging to remote sensing. *Global Ecology and Biogeography* 28, 1578–1596.
- Lembrechts, J.J., Aalto, J., Ashcroft, M.B., De Frenne, P., Kopecký, M., Lenoir, J., Luoto, M., Maclean, I.M.D., Roupsard, O., Fuentes-Lillo, E., García, R.A., Pellissier, L., Pitteloud, C., Alatalo, J.M., Smith, S.W., Björk, R.G., Muffler, L., Ratier Backes, A., Cesarz, S., Gottschall, F., Okello, J., Urban, J., Plichta, R., Svátek, M., Phartyal, S.S., Wipf, S., Eisenhauer, N., Puşcaş, M., Turtureanu, P.D., Varlagin, A., Dimarco, R.D., Jump, A.S., Randall, K., Dorrepaal, E., Larson, K., Walz, J., Vitale, L., Svoboda, M., Finger Higgins, R., Halbritter, A.H., Curasi, S.R., Klupar, I., Koontz, A., Pearce, W.D., Simpson, E., Stembkovski, M., Jessen Graae, B., Vedel Sørensen, M., Høye, T.T., Fernández Calzado, M.R., Lorite, J., Carbognani, M., Tomaselli, M., Forte, T. ai.G.W., Petraglia, A., Haesen, S., Somers, B., Van Meerbeek, K., Björkman, M.P., Hylander, K., Merinero, S., Gharun, M., Buchmann, N., Dolezal, J., Matula, R., Thomas, A.D., Bailey, J.J., Ghosn, D., Kazakis, G., Pablo, M.A., Kemppinen, J., Niittynen, P., Rew, L., Seipel, T., Larson, C., Speed, J.D.M., Ardö, J., Cannone, N., Guglielmin, M., Malfasi, F., Bader, M.Y., Canessa, R., Stanisci, A., Kreyling, J., Schmeddes, J., Teuber, L., Aschero, V., Čiliak, M., Mális, F., De Smedt, P., Govaert, S., Meeussen, C., Vangansbeke, P., Gigauro, K., Lamprecht, A., Pauli, H., Steinbauer, K., Winkler, M., Ueyama, M., Nuñez, M.A., Ursu, T.-M., Haider, S., Wedegärtner, R.E.M., Smljanić, M., Trouillier, M., Wilming, M., Altman, J., Brūna, J., Hederová, L., Macek, M., Man, M., Wild, J., Vittoz, P., Pärtel, M., Barančok, P., Kanka, R., Kollár, J., Palaj, A., Barros, A., Mazzolari, A.C., Batters, M., Boeckx, P., Benito Alonso, J.-L., Zong, S., Di Cecco, V., Sitková, Z., Tielbörger, K., Brink, L., Weigel, R., Homeier, J., Dahlberg, C.J., Medinets, S., Medinets, V., De Boeck, H.J., Portillo-Estrada, M., Verryck, L.T., Milbau, A., Daskalova, G.N., Thomas, H.J.D., Myers-Smith, I.H., Blonder, B., Stephan, J.G., Descombes, P., Zellweger, F., Frei, E.R., Heinesch, B., Andrews, C., Dick, J., Siebicke, L., Rocha, A., Senior, R.A., Rixen, C., Jimenez, J.J., Boike, J., Pauchard, A., Scholten, T., Scheffers, B., Klings, D., Basham, E.W., Zhang, J., Zhang, Z., Geron, C., Fazlioglu, F., Candan, O., Sallo Bravo, J., Hrbacek, F., Laska, K., Cremonese, E., Haase, P., Moyano, F.E., Rossi, C., Nijs, I., 2020. SoilTemp: A global database of near-surface temperature. *Global Change Biology* 26, 6616–6629.
- Moore, I.D., Burch, G.J., Mackenzie, D.H., 1988. Topographic effects on the distribution of surface soil water and the location of ephemeral gullies. *Transactions of the ASAE* 31, 1098–1107.
- Naafs, B.D.A., Gallego-Sala, A.V., Inglis, G.N., Pancost, R.D., 2017a. Refining the global branched glycerol dialkyl glycerol tetraether (brGDGT) soil temperature calibration. *Organic Geochemistry* 106, 48–56.
- Naafs, B.D.A., Inglis, G.N., Zheng, Y., Amesbury, M.J., Biester, H., Bindler, R., Blewett, J., Burrows, M.A., del Castillo Torres, D., Chambers, F.M., Cohen, A.D., Evershed, R.P., Feakins, S.J., Gaika, M., Gallego-Sala, A., Gandois, L., Gray, D.M., Hatcher, P.G., Honorio Coronado, E.N., Hughes, P.D.M., Huguet, A., Könönen, M., Laggoun-Défarge, F., Lähteenoja, O., Lamentowicz, M., Marchant, R., McClymont, E., Pontevedra-Pombal, X., Ponton, C., Pourmand, A., Rizzuti, A.M., Rochefort, L., Schellekens, J., De Vleeschouwer, F., Pancost, R.D., 2017b. Introducing global peat-specific temperature and pH calibrations based on brGDGT bacterial lipids. *Geochimica et Cosmochimica Acta* 208, 285–301.
- Naafs, B.D.A., Oliveira, A.S.F., Mulholland, A.J., 2021. Molecular dynamics simulations support the hypothesis that the brGDGT paleothermometer is based on homeoviscous adaptation. *Geochimica et Cosmochimica Acta* 312, 44–56.
- Naafs, B.D.A., Rohrsen, M., Inglis, G.N., Lähteenoja, O., Feakins, S.J., Collinson, M.E., Kennedy, E.M., Singh, P.K., Singh, M.P., Lunt, D.J., Pancost, R.D., 2018. High temperatures in the terrestrial mid-latitudes during the early Palaeogene. *Nature Geoscience* 11, 766–771.
- Novozamsky, I., Houbá, V.J.G., van Eck, R., van Vark, W., 1983. A novel digestion technique for multi-element plant analysis. *Communications in Soil Science and Plant Analysis* 14, 239–248.
- O'Brien, C.L., Robinson, S.A., Pancost, R.D., Sinninghe Damsté, J.S., Schouten, S., Lunt, D.J., Alsenz, H., Bornemann, A., Bottini, C., Brassell, S.C., Farnsworth, A., Forster, A., Huber, B.T., Inglis, G.N., Jenkyns, H.C., Linnert, C., Littler, K., Markwick, P., McAnena, A., Mutterlose, J., Naafs, B.D.A., Püttmann, W., Sluijs, A., van Helmond, N.A.G.M., Vellekoop, J., Wagner, T., Wrobel, N.E., 2017. Cretaceous sea-surface temperature evolution: Constraints from TEX<sub>86</sub> and planktonic foraminiferal oxygen isotopes. *Earth-Science Reviews* 172, 224–247.
- Oksanen, J., Blanchet, F.G., Friendly, M., Kindt, R., Legendre, P., McGlinn, D., Minchin, P.R., O'Hara, R.B., Simpson, G.L., Solymos, P., Stevens, M.H.H., Szoecs, E., Wagner, H., 2019. *Vegan: community ecology package*. R package version 2.5-6.
- Peterse, F., van der Meer, M.T.J., Schouten, S., Jia, G., Ossebaar, J., Blokker, J., Sinninghe Damsté, J.S., 2009. Assessment of soil n-alkane δD and branched tetraether membrane lipid distributions as tools for paleoelevation reconstruction. *Biogeosciences* 6, 2799–2807.
- Pitcher, A., Hopmans, E.C., Schouten, S., Sinninghe Damsté, J.S., 2009. Separation of core and intact polar archaeal tetraether lipids using silica columns: insights into living and fossil biomass contributions. *Organic Geochemistry* 40, 12–19.
- Quast, C., Pruesse, E., Yilmaz, P., Gerken, J., Schweer, T., Yarza, P., Peplies, J., Glöckner, F.O., 2013. The SILVA ribosomal RNA gene database project: improved data processing and web-based tools. *Nucleic Acids Research* 41, D590–D596.
- Schouten, S., Hopmans, E.C., Pancost, R.D., Sinninghe Damsté, J.S., 2000. Widespread occurrence of structurally diverse tetraether membrane lipids: Evidence for the ubiquitous presence of low-temperature relatives of hyperthermophiles. *Proceedings of the National Academy of Sciences* 97, 14421–14426.
- Schouten, S., Hopmans, E.C., Sinninghe Damsté, J.S., 2013. The organic geochemistry of glycerol dialkyl glycerol tetraether lipids: A review. *Organic Geochemistry* 54, 19–61.
- Seibert, J., Stendahl, J., Sørensen, R., 2007. Topographical influences on soil properties in boreal forests. *Geoderma* 141, 139–148.
- Sinninghe Damsté, J.S., Hopmans, E.C., Pancost, R.D., Schouten, S., Geenevasen, J.A.J., 2000. Newly discovered non-isoprenoid glycerol dialkyl glycerol tetraether lipids in sediments. *Chemical Communications* 1683–1684.
- Sinninghe Damsté, J.S., Ossebaar, J., Abbas, B., Schouten, S., Verschuren, D., 2009. Fluxes and distribution of tetraether lipids in an equatorial African lake: Constraints on the application of the TEX<sub>86</sub> paleothermometer and BIT index in lacustrine settings. *Geochimica et Cosmochimica Acta* 73, 4232–4249.
- Sinninghe Damsté, J.S., Rijpstra, W.I.C., Hopmans, E.C., Weijers, J.W.H., Foesel, B.U., Overmann, J., Dedysh, S.N., 2011. 13,16-dimethyl octacosanoic acid (iso-diabolic acid), a common membrane-spanning lipid of Acidobacteria subdivisions 1 and 3. *Applied and Environmental Microbiology* 77, 4147–4154.
- Sinninghe Damsté, J.S., Rijpstra, W.I.C., Hopmans, E.C., Foesel, B.U., Wüst, P.K., Overmann, J., Tank, M., Bryant, D.A., Dunfield, P.F., Houghton, K., Stott, M.B., 2014. Ether- and ester-bound iso-diabolic acid and other lipids in members of Acidobacteria subdivision 4. *Applied and Environmental Microbiology* 80, 5207–5218.
- Sinninghe Damsté, J.S., Rijpstra, W.I.C., Foesel, B.U., Huber, K.J., Overmann, J., Nakagawa, S., Kim, J.J., Dunfield, P.F., Dedysh, S.N., Villanueva, L., 2018. An overview of the occurrence of ether- and ester-linked iso-diabolic acid membrane lipids in microbial cultures of the Acidobacteria: implications for brGDGT paleoproxies for temperature and pH. *Organic Geochemistry* 124, 63–76.
- Stevenson, F.J., 1982. *Humus Chemistry: Genesis, Composition, Reactions*. John Wiley & Sons, New York, USA.
- Suzuki, R., Shimodaira, H., 2006. Pvcust: an R package for assessing the uncertainty in hierarchical clustering. *Bioinformatics* 22, 1540–1542.
- Tybirik, K., Nilsson, M.-C., Michelsen, A., Kristensen, H.L., Shevtsova, A., Strandberg, M. T., Johansson, M., Nielsen, K.E., Riis-Nielsen, T., Strandberg, B., Johnsen, I., 2000. Nordic *Empetrum* dominated ecosystems: function and susceptibility to environmental changes. *AMBIO: A Journal of the Human Environment* 29, 90–97.
- Tierney, J.E., Poulsen, C.J., Montañez, I.P., Bhattacharya, T., Feng, R., Ford, H.L., Hönisch, B., Inglis, G.N., Petersen, S.V., Sahoo, N., Tabor, C.R., Thirumalai, K., Zhu, J., Burls, N.J., Foster, G.L., Goddérís, Y., Huber, B.T., Ivany, L.C., Turner, S.K.,

- Lunt, D.J., McElwain, J.C., Mills, B.J.W., Otto-Bliesner, B.L., Ridgwell, A., Zhang, Y. G., 2020. Past climates inform our future. *Science* 370, 6517.
- van Reeuwijk, L.P., 2002. Technical Paper 09: Procedures for Soil Analysis, sixth ed. | ISRIC (WWW Document). URL <https://www.isric.org/documents/document-type/technical-paper-09-procedures-soil-analysis-6th-edition>.
- Véquaud, P., Derenne, S., Anquetil, C., Collin, S., Poulénard, J., Sabatier, P., Huguet, A., 2021. Influence of environmental parameters on the distribution of bacterial lipids in soils from the French Alps: implications for paleo-reconstructions. *Organic Geochemistry* 153, 104194.
- Walinga, I., Van Der Lee, J.J., Houba, V.J.G., Van Vark, W., Novozamsky, I., 1995. Digestion in tubes with H<sub>2</sub>SO<sub>4</sub>-salicylic acid- H<sub>2</sub>O<sub>2</sub> and selenium and determination of Ca, K, Mg, N, Na, P, Zn. In: Walinga, I., Van Der Lee, J.J., Houba, V.J.G., Van Vark, W., Novozamsky, I. (Eds.), *Plant Analysis Manual*. Springer, Netherlands, Dordrecht, pp. 7–45.
- Wang, M., Zong, Y., Zheng, Z., Man, M., Hu, J., Tian, L., 2018. Utility of brGDGTs as temperature and precipitation proxies in subtropical China. *Scientific Reports* 8. <https://doi.org/10.1038/s41598-017-17964-0>.
- Weijers, J.W.H., Schouten, S., Hopmans, E.C., Geenevasen, J.A.J., David, O.R.P., Coleman, J.M., Pancost, R.D., Sinninghe Damsté, J.S., 2006. Membrane lipids of mesophilic anaerobic bacteria thriving in peats have typical archaeal traits. *Environmental Microbiology* 8, 648–657.
- Weijers, J.W.H., Schouten, S., van den Donker, J.C., Hopmans, E.C., Sinninghe Damsté, J. S., 2007. Environmental controls on bacterial tetraether membrane lipid distribution in soils. *Geochimica et Cosmochimica Acta* 71, 703–713.
- Xiao, W., Xu, Y., Ding, S., Wang, Y., Zhang, X., Yang, H., Wang, G., Hou, J., 2015. Global calibration of a novel, branched GDGT-based soil pH proxy. *Organic Geochemistry* 89–90, 56–60.
- Yang, H., Lü, X., Ding, W., Lei, Y., Dang, X., Xie, S., 2015. The 6-methyl branched tetraethers significantly affect the performance of the methylation index (MBT') in soils from an altitudinal transect at Mount Shennongjia. *Organic Geochemistry* 82, 42–53.